

Ocean acidification of a coastal Antarctic marine microbial community reveals a critical threshold for CO₂ tolerance in phytoplankton productivity

Stacy Deppeler¹, Katherina Petrou², Kai G. Schulz³, Karen Westwood^{4,5}, Imogen Pearce⁴, John McKinlay⁴, and Andrew Davidson^{4,5}

¹Institute for Marine and Antarctic Studies, University of Tasmania, Private Bag 129, Hobart, Tasmania 7001, Australia

²School of Life Sciences, University of Technology Sydney, 15 Broadway, Ultimo, New South Wales 2007, Australia

³Centre for Coastal Biogeochemistry, Southern Cross University, Military Rd, East Lismore, NSW, 2480, Australia

⁴Australian Antarctic Division, Department of the Environment and Energy, 203 Channel Highway, Kingston, Tasmania 7050, Australia

⁵Antarctic Climate and Ecosystems Cooperative Research Centre, Private Bag 80, Hobart, Tasmania 7001, Australia

Correspondence to: Stacy Deppeler (stacy.deppeler@utas.edu.au)

Abstract.

High-latitude oceans are anticipated to be some of the first regions affected by ocean acidification. Despite this, the effect of ocean acidification on natural communities of Antarctic marine microbes is still not well understood. In this study we exposed an early spring, coastal marine microbial community in Prydz Bay to CO₂ levels ranging from ambient (343 μ atm) to 1641 μ atm in six 650 l minicosms. Productivity assays were performed to identify whether a CO₂ threshold existed that led to a change in primary productivity, bacterial productivity, and the accumulation of Chlorophyll *a* (Chl *a*) and particulate organic matter (POM) in the minicosms. In addition, photophysiological measurements were performed to identify possible mechanisms driving changes in the phytoplankton community. A critical threshold for tolerance to ocean acidification was identified in the phytoplankton community between 953 and 1140 μ atm. CO₂ levels \geq 1140 μ atm negatively affected photosynthetic performance and Chl *a*-normalised primary productivity (csGPP_{14C}), causing significant reductions in gross primary production (GPP_{14C}), Chl *a* accumulation, nutrient uptake, and POM production. However, there was no effect of CO₂ on C:N ratios. Over time, the phytoplankton community acclimated to high CO₂ conditions, showing a down-regulation of carbon concentrating mechanisms (CCMs) and likely adjusting other intracellular processes. Bacterial abundance initially increased in CO₂ treatments \geq 953 μ atm (days 3-5), yet gross bacterial production (GBP_{14C}) remained unchanged and cell-specific bacterial productivity (csBP_{14C}) was reduced. Towards the end of the experiment, GBP_{14C} and csBP_{14C} markedly increased across all treatments regardless of CO₂ availability. This coincided with increased organic matter availability (POC and PON) combined with improved efficiency of carbon uptake. Changes in phytoplankton community production could have negative effects on the Antarctic food web and the biological pump, resulting in negative feedbacks on anthropogenic CO₂ uptake. Increases in bacterial abundance under high CO₂ conditions may also increase the efficiency of the microbial loop, resulting in increased organic matter remineralisation and further declines in carbon sequestration.

1 Introduction

The Southern Ocean (SO) is a significant sink for anthropogenic CO₂ (Metzl et al., 1999; Sabine et al., 2004; Frölicher et al., 2015). Approximately 30% of anthropogenic CO₂ emissions have been absorbed by the world's oceans, of which 40% has been via the SO (Raven and Falkowski, 1999; Sabine et al., 2004; Khatiwala et al., 2009; Takahashi et al., 2009, 2012; Frölicher et al., 2015). While ameliorating CO₂ accumulation in the atmosphere, increasing oceanic CO₂ uptake alters the chemical balance of surface waters, with the average pH having already decreased by 0.1 units since pre-industrial times (Sabine et al., 2004; Raven et al., 2005). If anthropogenic emissions continue unabated, future concentrations of CO₂ in the atmosphere are projected to reach \sim 930 μatm by 2100 and peak at \sim 2000 μatm by 2250 (Meinshausen et al., 2011; IPCC, 2013). This will result in a further reduction of the surface ocean pH by up to 0.6 pH units, with unknown consequences to the marine microbial community (Caldeira and Wickett, 2003). High-latitude oceans have been identified as amongst the first regions to experience the negative effects of ocean acidification, causing potentially harmful reductions in the aragonite saturation state and a decline in the ocean's capacity for future CO₂ uptake (Sabine et al., 2004; Orr et al., 2005; McNeil and Matear, 2008; Fabry et al., 2009; Hauck and Völker, 2015). Marine microbes play a pivotal role in the uptake and storage of CO₂ in the ocean, through phytoplankton photosynthesis and vertical transport of biological carbon to the deep ocean (Longhurst, 1991; Honjo, 2004). As the buffering capacity of the SO decreases over time, the biological contribution to total CO₂ uptake is expected to increase in importance (Hauck et al., 2015; Hauck and Völker, 2015). Thus, it is necessary to understand the effects of high CO₂ on the productivity of the marine microbial community if we are to predict how they may affect ocean biogeochemistry in the future.

Phytoplankton primary production provides the food source to higher trophic levels and plays a critical role in the sequestration of carbon from the atmosphere into the deep ocean (Azam et al., 1983, 1991; Longhurst, 1991; Honjo, 2004; Fenchel, 2008; Kirchman, 2008). In Antarctic waters it is restricted to a short summer season and is characterised by intense phytoplankton blooms that can reach over 200 mg Chl *a* m⁻² (Smith and Nelson, 1986; Nelson et al., 1987; Wright et al., 2010). Relative to elsewhere in the SO, the continental shelf around Antarctica accounts for a disproportionately high percentage of annual primary productivity (Arrigo et al., 2008a). In coastal Antarctic waters, seasonal CO₂ variability can be up to 450 μatm over a year (Gibson and Trull, 1999; Boyd et al., 2008; Moreau et al., 2012; Roden et al., 2013; Tortell et al., 2014). Sea ice forms a barrier to outgassing of CO₂ in winter, causing supersaturation of the surface water to \sim 500 μatm . Intense primary productivity in summer rapidly draws down CO₂ to <100 μatm , making this region a significant CO₂ sink during summer months (Hoppema et al., 1995; Ducklow et al., 2007; Arrigo et al., 2008b).

Ocean acidification studies on individual phytoplankton species have reported differing trends in primary productivity and growth rates. Increased CO₂ enhanced rates of primary productivity (Wu et al., 2010; Trimborn et al., 2013) and growth (Sobrino et al., 2008; Tew et al., 2014; Baragi et al., 2015; Chen et al., 2015; King et al., 2015) in some diatom species, while others were unaffected (Chen and Durbin, 1994; Sobrino et al., 2008; Berge et al., 2010; Trimborn et al., 2013; Chen et al., 2015; Hoppe et al., 2015; King et al., 2015; Bi et al., 2017). In contrast, CO₂-related declines in primary productivity and growth rate have also been observed (Barcelos e Ramos et al., 2014; Hoppe et al., 2015; King et al., 2015; Shi et al., 2017), suggesting that responses to ocean acidification are largely species-specific. These differing responses among phytoplankton

species may also cause changes in the composition of phytoplankton communities (Trimborn et al., 2013). It is difficult to extrapolate the response of individual species to natural communities, as monospecific studies exclude interactions among species and trophic levels. Estimates of CO₂ tolerance under laboratory conditions may also be influenced by experimental acclimation periods (Trimborn et al., 2014; Hennon et al., 2015; Torstensson et al., 2015; Li et al., 2017a), differences in 5 experimental conditions (e.g. nutrients, light climate) (Hoppe et al., 2015; Hong et al., 2017; Li et al., 2017b), methods of CO₂ manipulation (Shi et al., 2009; Gattuso et al., 2010), as well as region-specific environmental adaptations (Schaum et al., 2012). Thus, investigations on natural communities are essential in order to better understand the outcome of these complex interactions.

The effects of ocean acidification on natural Antarctic phytoplankton communities is currently not well understood (Petrou 10 et al., 2016; Deppele and Davidson, 2017). Tolerance to CO₂ levels up to \sim 800 μatm have been reported for natural coastal communities in the West Antarctic Peninsula and Prydz Bay, East Antarctica (Young et al., 2015; Davidson et al., 2016). Although in Prydz Bay, when CO₂ levels exceeded 780 μatm , primary productivity declined and community composition shifted toward smaller, picoeukaryotes (Davidson et al., 2016; Thomson et al., 2016; Westwood et al., in press). In contrast, 15 Ross Sea phytoplankton communities responded to CO₂ levels \geq 750 μatm with an increase in primary productivity and abundance of large chain-forming diatoms, suggesting that as CO₂ increases in this region, diatoms may increase in dominance over the prymnesiophyte *Phaeocystis antarctica* (Tortell et al., 2008b; Feng et al., 2010). The paucity of information regarding the ocean acidification response of these Antarctic coastal phytoplankton communities highlights the need for further research 20 to determine region-specific tolerances and potential tipping points in community productivity and composition in Antarctica.

Bacteria play an essential role in the microbial food web through the remineralisation of nutrients from sinking particles 25 (Azam et al., 1991) and as a food source for heterotrophic nanoflagellates (Pearce et al., 2010). Bacterial populations respond to increases in phytoplankton primary productivity by increasing their productivity and abundance, with maximum abundance often occurring after the peak of the phytoplankton bloom (Pearce et al., 2007). High CO₂ levels have been observed to have either no effect on abundance and productivity (Grossart et al., 2006; Allgaier et al., 2008; Paulino et al., 2008; Baragi et al., 2015; Wang et al., 2016) or increase growth rate and production only during the post-bloom phase of an experiment (Grossart 30 et al., 2006; Sperling et al., 2013; Westwood et al., in press). Thus, bacterial communities appear to be relatively tolerant to ocean acidification, with bacterial growth indirectly affected by ocean acidification responses of the phytoplankton community (Grossart et al., 2006; Allgaier et al., 2008; Engel et al., 2013; Piontek et al., 2013; Sperling et al., 2013; Bergen et al., 2016).

Mesocosm experiments are an effective way of monitoring the community response of microbial assemblages to environmental changes. Experiments examining multiple species and trophic levels can provide responses that differ significantly from 35 mono-specific studies. Numerous mesocosm studies have now been performed, assessing the effect of ocean acidification on natural marine microbial communities around the world (e.g. Kim et al., 2006; Hopkinson et al., 2010; Riebesell et al., 2013; Paul et al., 2015; Bach et al., 2016; Bunse et al., 2016). Studies in the Arctic reported increases in phytoplankton primary productivity, growth, and organic matter concentration at CO₂ levels \geq 800 μatm under nutrient-replete conditions (Bellerby et al., 2008; Egge et al., 2009; Engel et al., 2013; Schulz et al., 2013), whilst the bacterial community was unaffected (Grossart et al., 2006; Allgaier et al., 2008; Paulino et al., 2008; Baragi et al., 2015). These studies also highlight the importance of

nutrient availability on the community response to elevated CO₂, with substantial differences in primary and bacterial productivity, Chlorophyll *a* (Chl *a*), and elemental stoichiometry observed between nutrient-replete and nutrient-limited conditions (Riebesell et al., 2013; Schulz et al., 2013; Sperling et al., 2013; Bach et al., 2016).

Previous community-level studies investigating the effects of ocean acidification on natural coastal marine microbial communities in East Antarctica reported declines in primary and bacterial productivity when CO₂ levels exceeded 780 μatm (Westwood et al., in press). To build upon the results of Westwood et al. (in press), a similar experimental design was utilised, with a natural marine microbial community from the same region exposed to CO₂ levels ranging from 343 to 1641 μatm in 650 l minocosms. The methods were refined in our study to include an acclimation period to the CO₂ treatment under low light. Rates of primary productivity, bacterial productivity, and the accumulation of particulate organic matter (POM) were examined to ascertain whether the threshold for tolerance to CO₂ was similar to that reported by Westwood et al. (in press), or if acclimation affected the community response to high CO₂. Photophysiological measurements were also undertaken to assess underlying mechanisms that caused shifts in phytoplankton community productivity.

2 Methods

2.1 Minicomm setup

Natural microbial assemblages were incubated in six 650 l polythene tanks (minicosms) housed in a temperature controlled shipping container (Fig. 1). All minicosms were acid washed with 10% vol:vol AR HCl, thoroughly rinsed with MilliQ water, and given a final rinse with seawater from the sampling site before use. The minicosms were filled with seawater taken amongst decomposing fast ice in Prydz Bay, at Davis Station, Antarctica (68° 35' S 77° 58' E) on 19th November 2014. Water was transferred by helicopter in multiple collections using a 720 l Bambi Bucket to fill a 7000 l polypropylene holding tank. Seawater was gravity fed into the minicomm tanks through Teflon lined hosing fitted with an in-line 200 μm Arkal filter to exclude metazooplankton. All minicosms were filled simultaneously to ensure uniform distribution of microbes in all tanks.

The ambient water temperature at the time of sampling in Prydz Bay was -1.0 °C. Tanks were temperature controlled to an average temperature of 0.0 °C, with a maximum range of ± 0.5 °C, through cooling of the shipping container and warming with two 300W aquarium heaters (Fluval) that were connected to a temperature control program via Carel temperature controllers. The contents of each tank were gently mixed by a shielded high density polyethylene auger, rotating at 15 rpm, and each tank was covered with a sealed acrylic lid.

Each tank was illuminated on a 19:5 h light:dark cycle by two 150W HQI-TS/NDL (Osram) metal halide lamps (transmission spectra: www.osram.com.au/media/resource/hires/335357/powerstar-hqi-ts-excellence-70-w-and-150-w—the-latest-innovation-in-quartz-tec.pdf). The light output was filtered by a light-scattering filter and a one quarter colour temperature (CT) blue filter (Arri) to convert the tungsten lighting to a daylight spectral distribution, attenuating wavelengths <500 nm by ~20% and >550 nm by ~40% (Davidson et al., 2016).

Similar to Schulz et al. (2017) the fugacity of carbon dioxide ($f\text{CO}_2$) in each tank was raised to the target concentration in a step-wise manner over the first 5 days of the incubation (Fig. 2, see below). During this acclimation, phytoplankton growth

in the tanks was slowed by attenuating the light intensity to $0.9 \pm 0.2 \mu\text{mol photons m}^{-2} \text{ s}^{-1}$ using two 90% neutral density (ND) filters (Arri).

At the conclusion of this CO_2 acclimation period, the light intensity was increased for 24 h through replacement of the two 90% ND filters with one 60% ND filter. The final light intensity was achieved on day 7 with a one quarter CT blue and a 5 light-scattering filter, which proved to be saturating for photosynthesis (see below).

Unless otherwise specified, samples were taken for analyses on days 1, 3, and 5 during the CO_2 acclimation period and every 2 days from day 8 to 18.

2.2 Carbonate chemistry measurements and calculations

Samples for carbonate chemistry measurements were collected daily from each minicoshm in 500 ml glass stoppered bottles 10 (Schott Duran) following the guidelines of Dickson et al. (2007). Sub-samples for dissolved inorganic carbon (DIC, 50 ml glass stoppered bottles) and pH on the total scale (pH_T , 100 ml glass stoppered bottles) measurements were gently pressure filtered ($0.2 \mu\text{m}$) with a peristaltic pump at a flow rate of $\sim 30 \text{ ml min}^{-1}$, similar to Bockmon and Dickson (2014).

DIC was measured by infra-red absorption on an Apollo SciTech AS-C3 analyzer equipped with a LICOR LI-7000 detector using triplicate 1.5 ml samples. The instrument was calibrated (and checked for linearity) within the expected DIC concentration range with five sodium carbonate standards (Merck Suprapur) that were dried for 2 hours at 230°C and prepared 15 gravimetrically in milliQ water ($18.2 \text{ M}\Omega \text{ cm}^{-1}$) at 25°C . Furthermore, daily measurements of certified reference material batch CRM127 (Dickson, 2010) were used for improved accuracy. Volumetrically measured DIC was converted to $\mu\text{mol kg}^{-1}$ using calculated density derived from known temperature and salinity. The typical precision among triplicate measurements was $< 2 \mu\text{mol kg}^{-1}$.

pH_T was measured spectrophotometrically (GBC UV-Vis 916) in a ten centimetre thermostated (25°C) cuvette using the pH indicator dye m-cresol purple (Acros Organics, 62625-31-4, Lot A0321770) following the approach described in Dickson et al. (2007), which included changes in sample pH due to dye addition. Contact with air was minimized by sample delivery, 20 dye addition, and mixing via a syringe pump (Tecan, Cavro XLP6000). Dye impurities and instrument performance were accounted for by applying a constant off-set ($+0.003 \text{ pH}$ units), determined by the comparison of measured and calculated pH_T (from known DIC and total alkalinity (TA), including silicate and phosphate) of CRM127. Typical measurement precision for 25 triplicates was 0.001 for higher and 0.003 for lower pH treatments. For further details see Schulz et al. (2017).

Carbonate chemistry speciation was calculated from measured DIC and pH_T . In a first step, at in situ measured salinities (WTW197 conductivity meter), practical alkalinity (PA) was calculated at 25°C using the dissociation constants for carbonic acid determined by Mehrbach et al. (1973) as refitted by Lueker et al. (2000). Then, total carbonate chemistry speciation was 30 calculated from measured DIC and calculated PA for in situ temperature conditions.

2.3 Carbonate chemistry manipulation

The $f\text{CO}_2$ in the minicosms was adjusted by additions of $0.22 \mu\text{m}$ -filtered natural seawater that was saturated by bubbling with AR grade CO_2 for ≥ 30 mins. In order to keep $f\text{CO}_2$ as constant as possible throughout the experiment, pH in each minicosm

was measured with a portable, NBS-calibrated probe (Mettler Toledo) in the morning before sampling and the afternoon, to estimate the necessary amount of DIC to be added. The required volume of CO₂ enriched seawater was then transferred into 1000 ml infusion bags and added to the individual minocosms at a rate of about 50 ml min⁻¹. After reaching target levels, the mean *f*CO₂ levels in the minocosms were 343, 506, 634, 953, 1140, and 1641 μatm (Table S1).

5 2.4 Light irradiance

Average light intensity in each minocosm tank was calculated by measuring light intensity in the empty tanks at three depths (top, middle, and near-bottom) and across each tank (left, middle, and right) using a Biospherical Instruments' Laboratory Quantum Scalar Irradiance Meter (QSL-101). The average light irradiance received by phytoplankton within each tank was calculated following the equation of Riley (1957) (Table 1). Incoming irradiance (\bar{I}_o) was calculated as the average light 10 intensity across the top of the tank. The average vertical light attenuation (K_d) was calculated as the slope from regression of the natural log of light intensity at all three depths, and mixed depth (Z_m) was the depth of the minocosm tanks (1.14 m).

Changes in vertical light attenuation due to increases in Chl *a* concentration throughout the experimental period were calculated from the equation in Westwood et al. (in press); $K_{d(biomass)} = 0.0451157 \times \text{Chl } a \text{ (mg m}^{-3}\text{)}$. Total light attenuation $K_{d(total)}$ in each tank at each sampling day was calculated by addition of K_d and $K_{d(biomass)}$.

15 2.5 Nutrient analysis

No nutrients were added to the minocosms during the experiment. Macronutrient samples were obtained from each minocosm following the protocol of Davidson et al. (2016). Seawater was filtered through 0.45 μm Sartorius filters into 50 ml Falcon tubes and frozen at -20 °C for analysis in Australia. Concentrations of ammonia, nitrate plus nitrite (NOx), soluble reactive phosphorus (SRP), and molybdate reactive silica (Silica) were determined using flow injection analysis by Analytical Services 20 Tasmania following Davidson et al. (2016).

2.6 Elemental analysis

Samples for POM analysis, particulate organic carbon (POC) and particulate organic nitrogen (PON), were collected following the method of Pearce et al. (2007). Equipment for sample preparation was soaked in Decon 90 (Decon Laboratories) for >2 days and thoroughly rinsed in MilliQ water before use. Forceps and cutting blades were rinsed in 100% acetone between 25 samples. Seawater was filtered through muffled 25 mm Sartorius Quartz microfibre filters until clogged. The filters were folded in half and frozen at -80 °C for analysis in Australia. Filters were thawed and opposite one-eighth sub-samples were cut and transferred into a silver POC cup (Elemental Analysis Ltd). Inorganic carbon was removed from each sample through addition of 20 μl of 2N HCl to each cup and drying at 60 °C for 36 h. When dry, each cup was folded shut, compressed into a pellet, and stored in desiccant until analysed at the Central Science Laboratory, University of Tasmania, using a Thermo Finnigan EA 30 1112 Series Flash Elemental Analyser.

2.7 Chlorophyll *a*

Seawater was collected from each minicommunity and a measured volume was filtered through 13 mm Whatman GF/F filters (maximum filtration time of 20 min). Filters were folded in half, blotted dry, and immediately frozen in liquid nitrogen for analysis in Australia. Chlorophyll *a* (Chl *a*) pigments were extracted, analysed by HPLC, and quantified following the methods of

5 Wright et al. (2010). Chl *a* was extracted from filters with 300 μ l dimethylformamide plus 50 μ l methanol, containing 140 ng apo-8'-carotenal (Fluka) internal standard, followed by bead beating and centrifugation to separate the extract from particulate matter. Extracts (125 μ l) were diluted to 80% with water and analysed on a Waters HPLC using a Waters Symmetry C8 column and a Waters 996 photodiode array detector. Chl *a* was identified by its retention time and absorption spectra compared to a mixed standard sample from known cultures (Jeffrey and Wright, 1997), run daily before samples. Peak integrations were performed using Waters Empower software, checked manually for corrections, and quantified using the internal standard method 10 (Mantoura and Repeta, 1997).

2.8 ^{14}C primary productivity

Primary productivity incubations were performed following the method of Westwood et al. (2010), based on the technique of Lewis and Smith (1983). This method incubated phytoplankton for 1 h, minimising respiratory losses of photo-assimilated

15 ^{14}C so that the uptake nearly approximated gross primary productivity (e.g. Dring and Jewson, 1982; González et al., 2008; Regaudie-de Gioux et al., 2014). Samples were analysed for total organic carbon (TO ^{14}C) content, thereby including any ^{14}C -labelled photosynthate leaked to the dissolved organic carbon (DO ^{14}C) pool (Regaudie-de Gioux et al., 2014).

For all samples, 5.92 MBq (0.16 mCi) of ^{14}C -sodium bicarbonate ($\text{NaH}^{14}\text{CO}_3$, PerkinElmer) was added to 162 ml of seawater from each minicommunity, creating a working solution of 37 kBq ml^{-1} . Aliquots of this working solution (7 ml) were then

20 added to glass scintillation vials and incubated for 1 h at 21 light intensities, ranging from 0 - 1412 $\mu\text{mol photons m}^{-2} \text{s}^{-1}$. The temperature within each of the vials was maintained at $-1.0 \pm 0.3^\circ\text{C}$ through water cooling of the incubation chamber. The reaction was terminated with the addition of 250 μl of 6N HCl and the vials were shaken for 3 hours at 200 rpm to remove dissolved inorganic carbon. Duplicate time zero (T_0) samples were set up in a similar manner to determine background radiation, with 250 μl of 6N HCl added immediately to quench the reaction without exposure to light. Duplicate 100% samples 25 were also performed to determine the activity of the working solution for each minicommunity. For each 100% sample, 100 μl of working solution was added to 7 ml 0.1M NaOH in filtered seawater to bind all ^{14}C . For radioactive counts, 10 ml Ultima Gold LLT scintillation cocktail (PerkinElmer) was added to each scintillation vial, shaken, and decays per minute (DPM) were counted in a PerkinElmer Tri-Carb 2910TR Low Activity Liquid Scintillation Analyzer with a maximum counting time set at 3 min.

30 DPM counts were converted into primary productivity following the equation of Steemann Nielsen (1952) (Table 1), using measured DIC concentrations (varying between ~ 2075 - $2400 \mu\text{mol kg}^{-1}$) and normalised to Chl *a* using minicommunity Chl *a* concentration (see above). Photosynthesis versus irradiance (PE) curves were modelled for each treatment following the equation of Platt et al. (1980) using the *Phytotools* package in R (Silsbe and Malkin, 2015; R Core Team, 2016). Photosynthetic param-

ter estimates included the light-saturated photosynthetic rate (P_{max}), maximum photosynthetic efficiency (α), photoinhibition rate (β), and saturating irradiance (E_k). Modelled Chl *a*-specific primary productivity ($csGPP_{14C}$) was calculated following the equation of Platt et al. (1980) using average minicommunity light irradiance (\bar{I}). Gross primary production rates (GPP_{14C}) in each tank were calculated from modelled $csGPP_{14C}$ and Chl *a* concentration (see above). Calculations and units for each parameter
5 are presented in Table 1.

2.9 Gross community productivity

Community photosynthesis and respiration rates were measured using custom-made mini-chambers. The system consisted of four, 5.1 ml glass vials with oxygen sensor spots (Pyroscience) attached on the inside of the vials using non-toxic silicon glue. The vials were sealed, ensuring any oxygen bubbles were omitted and all vials were stirred continuously using small
10 Teflon magnetic fleas to allow homogenous mixing of gases within the system during measurements. To improve the signal to noise ratio, seawater from each minicommunity was concentrated above a 0.8 μ m, 47 mm diameter polycarbonate membrane filter (Poretics) with gentle vacuum filtration and re-suspended in seawater from each minicommunity CO_2 treatment. Each chamber was filled with the cell suspension and placed in a temperature controlled incubator (0.0 ± 0.5 $^{\circ}C$). Light was supplied via
15 fluorescent bulbs above each chamber and light intensity calibrated using a 4π sensor. Oxygen optode spots were connected to a FireSting O_2 logger and data acquired using FireSting software (PyroScience). The optode was calibrated according to the manufacturer's protocol immediately prior to measurements using a freshly prepared sodium thiosulfate solution (10% w/w) and agitated filtered seawater (0.2 μ m) at experimental temperature for 0% and 100% air saturation values, respectively.
15 Oxygen concentration was recorded until a linear change in rate was established for each pseudoreplicate ($n = 4$).

Measurements were first recorded in the light (188 μ mol photons $m^{-2} s^{-1}$) and subsequently in the dark, with the initial
20 steeper portion of the slope used for a linear regression analysis to determine post-illumination (PI) respiration rate. Gross community production (GCP_{O_2}) was then calculated from dark PI respiration ($Resp_{O_2}$) and net community production (NCP_{O_2}) rates and normalised to Chl *a* concentration ($csGCP_{O_2}$, Table 1). Chl *a* content for each concentrated sample was determined by extracting pigments in 90% chilled acetone and incubating in the dark at 4 $^{\circ}C$ for 24 h. Chl *a* concentrations were determined using a spectrophotometer (Cary50: Varian) and calculated according to the equations of Jeffrey and Humphrey (1975),
25 modified by Ritchie (2006).

2.10 Chlorophyll *a* fluorescence

Photosynthetic efficiency of the microalgal community was measured via Chl *a* fluorescence using a Pulse Amplitude Modulated fluorometer (Water PAM, Walz). A 3 ml aliquot from each minicommunity was transferred into a quartz cuvette with continuous stirring to prevent cells from settling. To establish an appropriate dark adaptation period, several replicates were measured after
30 5, 10, 15, 20 and 30 min of dark adaptation, with the latter having the highest maximum quantum yield of PSII (F_v/F_m). Following dark adaptation, minimum fluorescence (F_0) was recorded before application of a high intensity saturating pulse of light (saturating pulse width = 0.8 s; saturating pulse intensity $>3,000$ μ mol photons $m^{-2} s^{-1}$), where maximum fluorescence (F_m) was determined. The maximum quantum yield of PSII was calculated from these two parameters (Schreiber,
30

2004). Following F_v/F_m , a five-step steady state light curve (SSLC) was conducted with each light level (130, 307, 600, 973, 1450 $\mu\text{mol photons m}^{-2} \text{ s}^{-1}$) applied for 5 min before recording the light-adapted minimum (F_t) and maximum fluorescence ($F_{m'}$) values. Each light step was spaced by a 30 sec dark 'recovery' period, before the next light level was applied. Three pseudoreplicate measurements were conducted on each minicommunity sample at 0.1 °C. Non-photochemical quenching (NPQ) of 5 Chl *a* fluorescence was calculated from F_m and $F_{m'}$ measurements. Relative electron transport rates (rETR) were calculated as the product of effective quantum yield ($\Delta F/F_{m'}$) and actinic irradiance (I_a). Calculations and units for each parameter are presented in Table 1.

2.11 Community carbon concentrating mechanism activity

To investigate the effects of CO₂ on carbon uptake, two inhibitors for carbonic anhydrase (CA) were applied to the 343 and 1641 μatm treatments on day 15: ethoxzolamide (EZA, Sigma), which inhibits both intracellular carbonic anhydrase (iCA) and extracellular carbonic anhydrase (eCA), and acetazolamide (AZA, Sigma), which blocks eCA only. Stock solutions of EZA (20 mM) and AZA (5 mM) were prepared in milliQ water, and the pH adjusted using NaOH to minimise pH changes when added to the samples. Before fluorometric measurements were made, water samples from the 343 and 1641 μatm CO₂ treatments were filtered into ≥ 10 and $< 10 \mu\text{m}$ fractions and aliquots were inoculated either with 50 μl of milliQ water adjusted with NaOH 10 (control) or 50 μM final concentration of chemical inhibitor (EZA and AZA). Fluorescence measurements of size fractionated control- and inhibitor-exposed cells were performed using the Water-PAM. A 3 ml aliquot of sample was transferred into a quartz cuvette, with stirring, and left in the dark for 30 min before maximum quantum yield of PSII (F_v/F_m) was determined 15 (as described above). Actinic light was then applied at 1450 $\mu\text{mol photons m}^{-2} \text{ s}^{-1}$ for 5 min before effective quantum yield of PSII ($\Delta F/F_{m'}$) was recorded. Three pseudoreplicate measurements were conducted on each minicommunity sample at 0.1 °C.

20 2.12 Bacterial abundance

Bacterial abundance was determined daily using a Becton Dickinson FACScan or FACSCalibur flow cytometer fitted with a 488 nm laser following the protocol of Thomson et al. (2016). Samples were pre-filtered through a 50 μm mesh (Nitex), stored at 4 °C in the dark, and analysed within 6 h of collection. Samples were stained for 20 min with 1:10,000 dilution SYBR-Green 25 I (Invitrogen) (Marie et al., 2005) and PeakFlow Green 2.5 μm beads (Invitrogen) were added to the sample as an internal fluorescence standard. Three pseudoreplicate samples were prepared from each minicommunity seawater sample. Samples were run for 3 min at a low flow rate ($\sim 12 \mu\text{l min}^{-1}$) and bacterial abundance was determined from side scatter (SSC) versus green (FL1) fluorescence bivariate scatter plots. The analysed volume was calibrated to the sample run time and each sample was run for precisely 3 min, resulting in an analysed volume of 0.0491 and 0.02604 ml on the FACSCalibur and FACScan, respectively. The volume analysed was then used to calculate final cell concentrations.

2.13 Bacterial productivity

Bacterial productivity measurements were performed following the Leucine incorporation by microcentrifuge method of Kirchman (2001). Briefly, 70 nM ^{14}C -Leucine (PerkinElmer) was added to 1.7 ml seawater from each minicosh in 2 ml polyethylene Eppendorf tubes and incubated for 2 h in the dark at 4 °C. Three pseudoreplicate samples were prepared from each minicosh 5 seawater sample. The reaction was terminated by the addition of 90 μl 100% trichloroacetic acid (TCA, Sigma) to each tube. Duplicate background controls were also performed following the same method, with 100% TCA added immediately before incubation. After incubation, samples were spun for 15 min at 12,500 rpm and the supernatant was removed. The cell pellet was resuspended into 1.7 ml ice-cold 5% TCA and spun again for 15 min at 12,500 rpm and the supernatant removed. The cell 10 pellet was then resuspended into 1.7 ml ice-cold 80% ethanol, spun for a further 15 min at 12,500 rpm and the supernatant removed. The cell pellet was allowed to dry completely before addition of 1 ml Ultima Gold scintillation cocktail (PerkinElmer). The Eppendorf tubes were placed into glass scintillation vials and DPMs were counted in a PerkinElmer Tri-Carb 2910TR 15 Low Activity Liquid Scintillation Analyzer with a maximum counting time of 3 min.

DPM counts were converted to ^{14}C -Leucine incorporation rates following the equation in Kirchman (2001) and used to calculate gross bacterial production (GBP ^{14}C), following Simon and Azam (1989). Bacterial production was divided by total 15 bacterial abundance to determine cell-specific bacterial productivity within each treatment (csBP ^{14}C). Calculations and units for each parameter are presented in Table 1.

2.14 Statistical analysis

The minicosh experimental design measured the microbial community growth in six unreplicated $f\text{CO}_2$ treatments. Therefore, sub-samples from each minicosh were within-treatment pseudoreplicates and thus, only provide a measure of the variability 20 of the within-treatment sampling and measurement procedures. We use pseudoreplicates as true replicates in order to provide an informal assessment of differences among treatments, noting that results must be treated as indicative and interpreted conservatively.

For all analyses, a linear or curved (quadratic) regression model was fitted to each CO_2 treatment over time using the *Stats* package in R (R Core Team, 2016) and an omnibus test of differences between the trends among CO_2 treatments over time was 25 assessed by ANOVA. This analysis ignored the repeated measures nature of the data set, which could not be modelled due to the low number of time points and an absence of replication at each time. For the CCM activity measurements, differences between treatments were tested by one-way ANOVA, followed by a post-hoc Tukey's test to determine which treatments differed. The significance level for all tests was set at < 0.05 .

3 Results

3.1 Carbonate chemistry

The $f\text{CO}_2$ of each treatment was modified in a step-wise fashion over 5 days to allow for acclimation of the microbial community to the changed conditions. Target treatment conditions were reached in all tanks by day 5, ranging from 343 to 1641 μatm , equating to an average pH_T of 8.10 to 7.45 (Fig. 2, Table S1), respectively. The initial seawater was calculated to have an $f\text{CO}_2$ of 356 μatm and a PA of 2317 $\mu\text{mol kg}^{-1}$, from a measured pH_T of 8.08 and DIC of 2187 $\mu\text{mol kg}^{-1}$ (Fig. S1, Table S2). One minicommunity was maintained close to these conditions (343 μatm) throughout the experiment as a control treatment.

3.2 Light climate

The average light irradiance for all CO_2 treatments is presented in Table S3. During the CO_2 acclimation period (days 1-5) the average light irradiance was $0.9 \pm 0.2 \mu\text{mol photons m}^{-2} \text{ s}^{-1}$ and was increased to $90.5 \pm 21.5 \mu\text{mol photons m}^{-2} \text{ s}^{-1}$ by day 8. The average vertical light attenuation (K_d) across all minicommunity tanks was 0.92 ± 0.2 . Increasing Chl a concentration over time in all CO_2 treatments increased $K_{d(\text{total})}$ from 0.96 ± 0.01 on day 1 to 3.53 ± 0.28 on day 18, resulting in a decline in average light irradiance within the minicommunities from 86.61 ± 20.5 to $35.97 \pm 9.3 \mu\text{mol photons m}^{-2} \text{ s}^{-1}$ between days 8-18.

3.3 Nutrients

Nutrient concentrations were similar across all treatments at the beginning of the experiment (Table S2) and did not change during the acclimation period (days 1-5). Ammonia concentrations were initially low ($0.95 \pm 0.18 \mu\text{M}$) and fell rapidly to concentrations below the limits of detection beyond day 12 in all treatments (Fig. S2). No differences in draw-down between CO_2 treatments were observed, and thus it was excluded from further analysis. NO_x fell from $26.2 \pm 0.74 \mu\text{M}$ on day 8 to concentrations below detection limits on day 18 (Fig. 3a), with the slowest draw-down in the 1641 μatm treatment. SRP concentrations were initially $1.74 \pm 0.02 \mu\text{M}$ and all CO_2 treatments followed a similar draw-down sequence to NO_x , reaching very low concentrations ($0.13 \pm 0.03 \mu\text{M}$) on day 18 in all treatments (Fig. 3b). In contrast, silica was replete in all treatments throughout the experiment falling from $60.0 \pm 0.91 \mu\text{M}$ to $43.6 \pm 2.45 \mu\text{M}$ (Fig. 3c). Draw-down of silica was exponential from day 8 onwards and followed a similar pattern to NO_x and SRP , with the highest silica draw-down in the 634 μatm and the least in the 1641 μatm treatment.

3.4 Particulate organic matter

Particulate organic carbon (POC) and nitrogen (PON) concentrations were initially low, 4.7 ± 0.15 and $0.5 \pm 0.98 \mu\text{M}$ respectively, and increased after day 8 in all treatments (Fig. 4a-b). The accumulation of POC and PON was effectively the reciprocal of the draw-down of nutrients (see above), being lowest in the high CO_2 treatments ($\geq 1140 \mu\text{atm}$) and highest in the 343 and 643 μatm treatments. Rates of POC and PON accumulation were both affected by nutrient exhaustion, with declines in the 343 and 634 μatm treatments between days 16 to 18. POC and PON concentrations on day 18 were highest in the 953 μatm

treatment. The ratio of POC to PON (C:N) was similar for all treatments, declining from 8.0 ± 0.38 on day 8 to 5.7 ± 0.28 on day 16 (Fig. 4c). The slowest initial decline in C:N ratio occurred in the 1641 μatm treatment, displaying a prolonged lag until day 10, after which it decreased to values similar to all other treatments. Nutrient exhaustion on day 18 coincided with an increase in the C:N ratio in all treatments, with C:N ratios >10 in the 343, 634, and 953 μatm treatments and lower C:N ratios (8.6-6.7) in the 506, 1140, and 1641 μatm treatments.

5 3.5 Chlorophyll *a*

Chl *a* concentrations were low at the beginning of the experiment, $0.91 \pm 0.16 \mu\text{g l}^{-1}$ and increased in all treatments after day 8 (Fig. 5a). Chl *a* accumulation rates were similar amongst treatments $\leq 634 \mu\text{atm}$ until day 14, with slightly higher Chl *a* concentration in the 506 and 634 μatm treatments on day 16 compared to the control treatment. By day 18, only the 503 μatm treatment remained higher than the control. Chl *a* accumulation rates in the 953 and 1140 μatm treatments were initially 10 slow but increased after day 14, with Chl *a* concentrations similar to the control on days 16-18. The highest CO₂ treatment (1641 μatm) had the slowest rates of Chl *a* accumulation, displaying a lag in growth between days 8-12, after which Chl *a* concentration increased but remained lower than the control. Rates of Chl *a* accumulation slowed between days 16 and 18 in 15 all treatments except 1641 μatm , coinciding with nutrient limitation. At day 18, the highest Chl *a* concentration was in the 506 μatm exposed treatment and lowest at 1641 μatm .

The omnibus test among CO₂ treatments of trends in Chl *a* over time indicated that the accumulation of Chl *a* in at least one treatment differed significantly from that of the control ($F_{5,23} = 5.5$, $p = 0.002$; Table S4). Examination of individual coefficients from the model revealed that only the highest CO₂ treatment, 1641 μatm , was significantly different from the control at the 5% level.

20 3.6 ¹⁴C primary productivity

During the CO₂ and light acclimation phase of the experiment (days 1-8) all treatments displayed a steady decline in the maximum photosynthetic rate (P_{max}) and the maximum photosynthetic efficiency (α) to levels on day 8 approximately half of those at the beginning of the experiment, suggesting cellular acclimation to the light conditions (Fig. S3a-b). Thereafter, relative 25 to the control, P_{max} and α were lowest in CO₂ levels $\geq 953 \mu\text{atm}$ and $\geq 634 \mu\text{atm}$, respectively. Rates of photoinhibition (β) and saturating irradiance (E_k) were variable and did not differ among treatments (Fig. S3c-d). The average E_k across all treatments was $28.7 \pm 8.6 \mu\text{mol photons m}^{-2} \text{s}^{-1}$, indicating that the light intensity in the minicoms was saturating for photosynthesis (see above) and not inhibiting ($\beta < 0.002 \text{ mg C (mg Chl } a)^{-1} (\mu\text{mol photons m}^{-2} \text{s}^{-1})^{-1} \text{ h}^{-1}$).

Chl *a*-specific primary productivity (csGPP_{14C}) and gross primary production (GPP_{14C}) was low during the CO₂ acclimation (days 1-5) and increased with increasing light climate after day 5. Rates of csGPP_{14C} in treatments $\geq 634 \mu\text{atm}$ CO₂ were 30 consistently lower than the control between days 8-16, with the lowest rates in the highest CO₂ treatment (1641 μatm) (Fig. 6a). Rates of GPP_{14C} in treatments ≤ 953 were similar between days 8-16, with the 343 (control), 506, and 953 μatm treatments increasing to $46.7 \pm 0.34 \mu\text{g C l}^{-1} \text{ h}^{-1}$ by day 18 (Fig. 5b). Compared to these treatments, GPP_{14C} in the 634 μatm treatment

was lower on day 18, only reaching $39.7 \mu\text{g C l}^{-1} \text{ h}^{-1}$, possibly due to the concurrent limitation of NO_x in this treatment on day 16 (see above).

The omnibus test among tanks of the trends in CO₂ treatments over time indicated that GPP_{14C} in at least one treatment differed significantly from the control ($F_{5,23} = 4.9$, $p = 0.003$; Table S5). Examination of the significance of individual curve terms revealed this manifested as differences between the 1140 and 1641 μatm treatments and the control group at the 5% level. No other curves were different from the control. In particular, GPP_{14C} in the 1641 μatm treatment was much lower until day 12, after which it increased steadily until day 16. Between days 16-18, a substantial increase in GPP_{14C} was observed in this treatment, subsequently resulting in a rate on day 18 that was similar to the 1140 μatm treatment ($36.3 \pm 0.08 \mu\text{g C l}^{-1} \text{ h}^{-1}$). Although, these treatments never reached rates of GPP_{14C} as high as the control.

10 3.7 Gross community productivity

Productivity of the phytoplankton community increased over time in all CO₂ treatments, however there were clear differences in the timing and magnitude of this increase between treatments (Fig. 6b). A CO₂ effect was evident on day 12, where Chl *a*-normalised gross O₂ productivity rates (csGCP_{O₂}) increased with increasing CO₂ level, ranging from 19.5 - 248 mg O₂ (mg Chl *a*)⁻¹ h⁻¹. After day 12, the communities in CO₂ treatments $\leq 634 \mu\text{atm}$ continued to increase their rates 15 of csGCP_{O₂} until day 18 ($97.7 \pm 17.0 \text{ mg O}_2 \text{ (mg Chl } a\text{)}^{-1} \text{ h}^{-1}$). The 953 and 1140 μatm CO₂ treatments peaked on day 12 (90.4 and 126 mg O₂ (mg Chl *a*)⁻¹ h⁻¹, respectively) and then declined on day 14 to rates similar to the control treatment. In contrast, the 1641 μatm treatment maintained high rates of csGCP_{O₂} from days 12-14 ($258 \pm 13.8 \text{ mg O}_2 \text{ (mg Chl } a\text{)}^{-1} \text{ h}^{-1}$), coinciding with the recovery of photosynthetic health (F_v/F_m , see below) and the initiation of growth in this treatment (see above). After this time, rates of csGCP_{O₂} declined in this treatment to rates similar to the control. Despite these differences in 20 csGCP_{O₂}, there was no significant difference between gross community production (GCP_{O₂}) among CO₂ treatments (Fig. 5c).

3.8 Community photosynthetic efficiency

Community maximum quantum yield of PSII (F_v/F_m) showed a dynamic response over the duration of the experiment (Fig. 7). Values initially increased during the low light CO₂ adjustment period, but declined by day 8 when irradiance levels had increased. Between days 8-14, differences were evident in the photosynthetic health of the phytoplankton community across the 25 CO₂ treatments, although by day 16 these differences had disappeared. Steady state light curves revealed that the community photosynthetic response did not change with increasing CO₂. Effective quantum yield of PSII ($\Delta F/F_{m'}$) and NPQ showed no variability with CO₂ treatment (Fig. S5, S6). There was however, a notable decline in overall NPQ in all tanks with time, indicating an adjustment to the higher light conditions. Relative electron transport rates (rETR) showed differentiation with respect to CO₂ at high light ($1450 \mu\text{mol photons m}^{-2} \text{ s}^{-1}$) on days 10-12. However, as seen with the F_v/F_m response, this 30 difference was diminished by day 18 (Fig. S7).

3.9 Community CCM activity

There was a significant decline in the effective quantum yield of PSII ($\Delta F/F_{m'}$) with the addition of the iCA and eCA inhibitor EZA to both the large ($\geq 10 \mu\text{m}$, $p = 0.02$) and small ($< 10 \mu\text{m}$, $p < 0.001$) size fractions of the phytoplankton community exposed to the control (343 μatm) CO_2 treatment (Fig. 8). The addition of EZA to cells under high CO_2 (1641 μatm) had no effect on $\Delta F/F_{m'}$ for either size fraction. However, in the case of the small cells under high CO_2 (Fig. 8b), $\Delta F/F_{m'}$ was the same as that measured in the control CO_2 in the presence of EZA. The addition of AZA, which inhibits eCA only, had no effect for either CO_2 treatments in the large celled community. In contrast, there was a significant decline in $\Delta F/F_{m'}$ in the smaller fraction in the control CO_2 treatment ($p < 0.001$), but no effect of AZA addition under high CO_2 . Again, the high CO_2 cells exhibited the same $\Delta F/F_{m'}$ as those measured under the control CO_2 in the presence of AZA.

10 3.10 Bacterial abundance

During the 8 day acclimation period, bacterial abundance in treatments $\geq 634 \mu\text{atm}$ increased with increasing CO_2 , reaching $26.0\text{--}32.4 \times 10^7 \text{ cells l}^{-1}$, and remaining high until day 13 (Fig. 9a). Between days 7–13, bacterial abundances in CO_2 treatments $\geq 953 \mu\text{atm}$ were higher than the control. In contrast, abundance remained constant in treatments $\leq 506 \mu\text{atm}$ ($20.6 \pm 1.4 \times 10^7 \text{ cells l}^{-1}$) until day 11. Cell numbers rapidly declined in all treatments after day 12, finally stabilising at $0.5 \pm 0.2 \times 10^7 \text{ cells l}^{-1}$. An omnibus test among CO_2 treatments of the trends in bacterial abundance over time showed that changes in abundance in at least one treatment differed significantly from the control ($F_{5,185} = 9.8$, $p < 0.001$; Table S6). Examination of individual coefficients from the model revealed that CO_2 treatments $\geq 953 \mu\text{atm}$ were significantly different from the control at the 5% level.

3.11 Bacterial productivity

20 Gross bacterial production ($\text{GBP}_{14\text{C}}$) was low in all CO_2 treatments ($0.2 \pm 0.03 \mu\text{g C l}^{-1} \text{ h}^{-1}$) and changed little during the first 5 days of incubation (Fig. 9b). Thereafter it increased, coinciding with exponential growth in the phytoplankton community. The most rapid increase in $\text{GBP}_{14\text{C}}$ was observed in the $634 \mu\text{atm}$ treatment, resulting in a rate twice that of all other treatments by day 18 ($2.1 \mu\text{g C l}^{-1} \text{ h}^{-1}$). No difference was observed among other treatments, all of which increased to an average rate of $1.1 \pm 0.1 \mu\text{g C l}^{-1} \text{ h}^{-1}$ by day 18. Cell-specific bacterial productivity ($\text{csBP}_{14\text{C}}$) was low in all treatments ($1.2 \pm 0.5 \text{ fg C l}^{-1} \text{ h}^{-1}$) until day 14, with slower rates in treatments $\geq 953 \mu\text{atm}$, likely due to high cell abundances observed in these treatments (Fig. S8). It then increased from day 14, coinciding with a decline in bacterial abundance. Rates of $\text{csBP}_{14\text{C}}$ did not differ among treatments until day 18, when the rate in the $634 \mu\text{atm}$ treatment was higher than all other treatments ($0.5 \mu\text{g C cell}^{-1} \text{ l}^{-1} \text{ h}^{-1}$).

4 Discussion

Our study of a natural Antarctic phytoplankton community identified a critical threshold for tolerance of CO₂ between 953 and 1140 μatm , above which photosynthetic health was negatively affected and rates of carbon fixation and Chl *a* accumulation declined. Low rates of primary productivity also led to declines in nutrient uptake rates and POM production, although there 5 was no effect of CO₂ on C:N ratios, indicating that ocean acidification effects on the phytoplankton community did not modify POM stoichiometry. Assessing the temporal trends of Chl *a*, GPP¹⁴C, and PON against CO₂ treatment revealed that the down- turn in these parameters occurred between 634 and 953 μatm $f\text{CO}_2$ and could be discerned following ≥ 12 days incubation (Fig. 10). On the final day of the experiment (day 18), this CO₂ threshold was less clear and likely confounded by the effects 10 of nutrient limitation (Westwood et al., *in press*). In contrast, bacterial productivity was unaffected by increased CO₂. Instead, their production coincided with increased organic matter supply from phytoplankton primary productivity. In the following sections these effects will be investigated further, with suggestions for possible mechanisms that may be driving the responses observed.

4.1 Ocean acidification effects on phytoplankton productivity

The results of this study suggest that exposing phytoplankton to high CO₂ levels can decouple the two stages of photosynthesis 15 (but also see discussion below). At CO₂ levels $\geq 1140 \mu\text{atm}$, Chl *a*-specific oxygen production (csGCP_{O₂}) increased strongly yet displayed the lowest rates of Chl *a*-specific carbon fixation (csGPP¹⁴C, Fig. 6). This mismatch in oxygen production and carbon fixation is likely due to the two-stage process in the photosynthetic fixation of carbon (reviewed in Behrenfeld et al., 2004). In the first stage, light-dependent reactions occur within the chloroplast, converting light energy (photons) into the 20 cellular energy products, adenosine triphosphate (ATP) and nicotinamide adenine dinucleotide phosphate (NADPH), producing O₂ as a by-product. This cellular energy is then utilised in a second, light-independent pathway, which uses the carbon-fixing enzyme RuBisCo to convert CO₂ into sugars through the Calvin Cycle. However, under certain circumstances the relative pool of energy may also be consumed in alternative pathways, such as respiration and photoprotection (Behrenfeld et al., 2004; Gao and Campbell, 2014). Increases in energy requirements for these alternate pathways have been demonstrated, 25 where measurements of maximum photosynthetic rates (P_{max}) and photosynthetic efficiency (α) display changes that result in no change to saturating irradiance levels (E_k) (Behrenfeld et al., 2004, 2008; Halsey et al., 2010). This "E_k-independent variability" was evident in our study, where decreases in P_{max} and α were observed in the high CO₂ treatments, while E_k remained unaffected (Fig. S3).

This highlights an important tipping point in the phytoplankton community's ability to cope with the energetic requirements 30 for maintaining efficient productivity under high CO₂. While studies on individual phytoplankton species have reported decoupling of the photosynthetic pathway under conditions of stress, to date, no studies on natural phytoplankton communities have reported this response. Under laboratory conditions, stresses such as nutrient limitation (Halsey et al., 2010) or a combination of high CO₂ and light climate (Hoppe et al., 2015; Liu et al., 2017) have been shown to induce such a response, where isolated phytoplankton species possess higher energy requirements for carbon fixation. In our study, the phytoplankton community

experienced a dynamic light climate due to continuous gentle mixing of the minicommunity contents, and although nutrients weren't limiting, the phytoplankton in the higher CO₂ treatments did show lower csGPP_{14C} rates (Fig. 6a), which could be linked to higher energy demand for light-independent processes. Since nutrients were replete and not a likely source of stress, it follows that CO₂ and light were likely the only sources of stress on this community.

5 Increased respiration rates could account for the decreased carbon fixation rates measured. Thus far, respiration rates are commonly reported as either unaffected or lower under increasing CO₂ (Hennon et al., 2014; Trimborn et al., 2014; Spilling et al., 2016). This effect is generally attributed to declines in cellular energy requirements, via processes such as down-regulation of CCMs, which can result in observed increases to rates of production (Spilling et al., 2016). Despite this, decreased growth rates have been linked to enhanced respiratory carbon loss at high CO₂ levels (800-1000 μatm) (Gao et al., 2012b). The 10 contribution of community respiration rates to csGCP_{O₂} was high and increased with increasing CO₂ (Fig. S4). However, respiration rates were generally proportional to the increase in O₂ production (i.e. the ratio of production to respiration remained constant across CO₂ conditions), making it unlikely to be a significant contributor to the decline in carbon fixation. Instead, high respiration rates were possibly a result of heterotrophic activity.

15 It has been suggested that the negative effects of ocean acidification are predominantly due to the decline in pH and not the increase in CO₂ concentration (e.g. McMinn et al., 2014; Coad et al., 2016). A decline in pH with ocean acidification increases the hydrogen ion (H⁺) concentration in the seawater and is likely to make it increasingly difficult for phytoplankton cells to maintain cellular homeostasis. Metabolic processes, such as photosynthesis and respiration, impact on cellular H⁺ fluxes between compartments, making it necessary to temporarily balance internal H⁺ concentrations through H⁺ channels (Taylor et al., 2012). Under normal oceanic conditions (pH \sim 8.1), when the extracellular environment is above pH 7.8, excess H⁺ 20 ions generated within the cell are able to passively diffuse out of the cell through these H⁺ channels. However, a lowering of the oceanic pH below 7.8 is likely to halt this passive removal of internal H⁺, requiring the utilisation of energy-intensive proton pumps (Taylor et al., 2012), and thus potentially reducing the energy pool available for carbon fixation. While not well understood, these H⁺ channels may also perform important cellular functions, such as nutrient uptake, cellular signalling, and defense (Taylor et al., 2012). Our results are consistent with this idea of a critical pH threshold, as significant declines in 25 GPP_{14C} were observed in treatments \geq 1140 μatm (Fig. 10), the CO₂ treatments where the pH ranged from 7.69-7.45 (Fig. 2).

Despite the initial stress of high CO₂ between days 8-12, the phytoplankton community displayed a strong ability to adapt to these conditions. The CO₂-induced reduction in F_v/F_m showed a steady recovery between days 12 and 16, with all treatments displaying similar high F_v/F_m at day 16 (0.68-0.71, Fig. 7). This recovery in photosynthetic health suggests that the phytoplankton community was able to acclimate to the high CO₂ conditions, possibly through cellular acclimation, changes 30 in community structure, or most likely, a combination of both. Cellular acclimations were observed in our study. A lowering of NPQ and a minimisation of the CO₂-related response to photoinhibition (rETR) at high light intensity suggested that PSII was being down-regulated to adjust to a higher light climate (Fig. S6, S7). Decreased energy requirements for carbon fixation were also observed in the photosynthetic pathway, resulting in increases to GPP_{14C} and Chl *a* accumulation rates (Fig. 5). Acclimation to increased CO₂ has been reported in a number of studies, resulting in shifts in carbon and energy utilisation 35 (Sobrino et al., 2008; Hopkinson et al., 2010; Hennon et al., 2014; Trimborn et al., 2014; Zheng et al., 2015). Numerous photo-

physiological investigations on individual phytoplankton species also report species-specific tolerances to increased CO₂ (Gao et al., 2012a; Gao and Campbell, 2014; Trimborn et al., 2013, 2014) and a general trend toward smaller-celled communities with increased CO₂ has been reported in ocean acidification studies globally (Schulz et al., 2017). Changes in community structure were observed with increasing CO₂, with taxon-specific thresholds of CO₂ tolerance (Hancock et al., 2017). Within 5 the diatom community, the response was also related to size, leading to an increase in abundance of small (<20 µm) diatoms in the higher CO₂ treatments ($\geq 953 \mu\text{atm}$). Therefore, the community acclimation observed is likely driven by an increase in growth of more tolerant species.

It is often suggested that the down-regulation of CCMs help to moderate the sensitivity of phytoplankton communities to increasing CO₂. The carbon-fixing enzyme RuBisCO has a low affinity for CO₂ that is compensated for through CCMs 10 that actively increase the intracellular CO₂ (Raven, 1991; Badger, 1994; Badger et al., 1998; Hopkinson et al., 2011). This process requires additional cellular energy (Raven, 1991) and numerous studies have suggested that the energy savings from down-regulation of CCMs in phytoplankton could explain increases in rates of primary productivity at elevated CO₂ levels 15 (e.g. Cassar et al., 2004; Tortell et al., 2008b, 2010; Trimborn et al., 2013; Young et al., 2015). In Antarctic phytoplankton communities, Young et al. (2015) showed that the energetic costs of CCMs are low and any down-regulation at increased CO₂ 20 would provide little benefit. We found that the CCM component carbonic anhydrase (CA) was utilised by the phytoplankton community at our control CO₂ level (343 µatm), and was down-regulated at high CO₂ (1641 µatm, Fig. 8). Yet we saw no promotion of primary productivity that coincided with this down-regulation. Thus, our data support the previous studies showing that increased CO₂ may alleviate energy supply constraints but does not necessarily lead to increased rates of carbon 25 fixation (Rost et al., 2003; Cassar et al., 2004; Riebesell, 2004).

Furthermore, size-specific differences in phytoplankton CCM utilisation were observed. The absence of eCA activity in 30 the large phytoplankton ($\geq 10 \mu\text{m}$, Fig. 8a) suggests that bicarbonate (HCO₃⁻) was the dominant carbon source used by this fraction of the phytoplankton community (Burkhardt et al., 2001; Tortell et al., 2008a). This is not surprising as direct HCO₃⁻ uptake has been commonly reported among Antarctic phytoplankton communities (Cassar et al., 2004; Tortell et al., 2010). On the other hand, the small phytoplankton (<10 µm, Fig. 8b) seem to have used both iCA and eCA, implying carbon 25 for photosynthesis was sourced through both extracellular conversion of HCO₃⁻ to CO₂ and direct HCO₃⁻ uptake (Rost et al., 2003). Despite these patterns, CCM activity in this study was only determined via Chl *a* fluorescence, and therefore direct measurement of light-dependent reactions in photosynthesis. This imposes limitations to the interpretability of this particular data set, as CA is involved primarily in carbon acquisition, which occurs during photosynthetic reactions that are independent 30 of light.

The presence of iCA has also been proposed as a possible mechanism for increased sensitivity of phytoplankton to decreased pH conditions. Satoh et al. (2001) found that the presence of iCA caused strong intracellular acidification and inhibition of carbon fixation when a CO₂-tolerant iCA-expressing algal species was transferred from ambient conditions to very high CO₂ (40%). Down-regulation of iCA through acclimation in a 5% CO₂ treatment eliminated this response, with similar tolerance 35 observed in an algal species with low ambient iCA activity. Thus, the down-regulation of iCA activity at high CO₂, as was seen

in our study, may not only decrease cellular energy demands but may also be operating as a cellular protection mechanism, allowing the cell to maintain intracellular homeostasis.

Contrary to the high CO₂ treatments, the phytoplankton community appeared to tolerate CO₂ levels up to 953 μatm , identifying a CO₂ threshold. Between days 8-14 we observed a small and insignificant CO₂-related decline in F_v/F_m, GPP¹⁴C, 5 and Chl *a* accumulation between the 343-953 μatm treatments (Fig. 7, 10). Tolerance of CO₂ levels up to \sim 1000 μatm has often been observed in natural phytoplankton communities in regions exposed to fluctuating CO₂ levels. In these communities, increasing CO₂ often had no effect on primary productivity (Tortell et al., 2000; Tortell and Morel, 2002; Tortell et al., 2008b; Hopkinson et al., 2010; Tanaka et al., 2013; Sommer et al., 2015; Young et al., 2015; Spilling et al., 2016) or growth (Tortell et al., 2008b; Schulz et al., 2013), although an increase in primary production has been observed in some instances (Riebesell, 10 2004; Tortell et al., 2008b; Egge et al., 2009; Tortell et al., 2010; Hoppe et al., 2013; Holding et al., 2015). These differing responses may be due to differences in community composition, nutrient supply, or ecological adaptations of the phytoplankton community in the region studied. They may also be due to differences in the experimental methods, especially the range of 15 CO₂ concentrations employed (Hancock et al., 2017); the mechanism used to manipulate CO₂ concentrations; the duration of the acclimation and incubation; the nature and volume of the mesocosms used; and the extent to which higher trophic levels are screened from the mesocosm contents (see Davidson et al., 2016).

Previous studies in Prydz Bay report a tolerance of the phytoplankton community to CO₂ levels up to 750 μatm (Davidson et al., 2016; Thomson et al., 2016; Westwood et al., in press). Although these experiments differed in nutrient concentration, community composition, and CO₂ manipulation from ours, when taken together, these studies demonstrate consistent CO₂ effects throughout the Antarctic summer season and across years in this location. The most likely reason for this high tolerance 20 is that these communities are already exposed to highly variable CO₂ conditions. CO₂ naturally builds beneath the sea ice in winter, when primary productivity is low (Perrin et al., 1987; Legendre et al., 1992), and is rapidly depleted during spring and summer by phytoplankton blooms, resulting in annual *f*CO₂ fluctuations between \sim 50-500 μatm (Gibson and Trull, 1999; Roden et al., 2013). Thus, variable CO₂ environments appear to promote adaptations within the phytoplankton community to manage the stress imposed by fluctuating CO₂.

25 Changes in POM production and C:N ratio in phytoplankton communities can have significant effects on carbon sequestration and change their nutritional value for higher trophic levels (Finkel et al., 2010; van de Waal et al., 2010; Polimene et al., 2016). We observed a decline in particulate organic matter production (POM) at CO₂ levels \geq 1140 μatm (Fig. 10), while changes in organic matter stoichiometry (C:N ratio) appeared to be predominantly controlled by nutrient consumption (Fig. 4). Increases in POM production were similar to Chl *a* accumulation, with declines in high CO₂ treatments (\geq 1140 μatm) due 30 to low rates of primary productivity. Carbon overconsumption has been reported in some natural phytoplankton communities exposed to increased CO₂, resulting in observed or inferred increases in the particulate C:N ratio (Riebesell et al., 2007; Engel et al., 2014). While in our study the C:N ratio did decline to below the Redfield Ratio during exponential growth, it remained within previously reported C:N ratios of coastal phytoplankton communities in this region (Gibson and Trull, 1999; Pasquer et al., 2010). However, as we did not analyse the elemental composition of dissolved inorganic matter, carbon overconsumption 35 cannot be completely ruled out (Kähler and Koeve, 2001). Therefore, it is difficult to say whether or not changes in primary pro-

ductivity will affect organic matter stoichiometry in this region, particularly as any resultant long-term changes in community composition to more CO₂-tolerant taxa may also have an effect (Finkel et al., 2010).

4.2 Ocean acidification effects on bacterial productivity

In contrast to the phytoplankton community, bacteria were tolerant of high CO₂ levels. The low bacterial productivity and abundance of the initial community is characteristic of the post-winter bacterial community in Prydz Bay where their growth is limited by organic nutrient availability (Pearce et al., 2007). Whilst an increase in cell abundance was observed at CO₂ levels $\geq 634 \mu\text{atm}$ (Fig. 9a), it was possible that this response was driven by a decline in grazing by heterotrophs (Thomson et al., 2016; Westwood et al., in press) instead of a direct CO₂-related promotion in bacterial growth. The subsequent decline in abundance was likely due to top-down control from the heterotrophic nanoflagellate community, which displayed an increase in abundance at this time (Hancock et al., 2017). Bacterial tolerance to high CO₂ has been reported previously in this region (Thomson et al., 2016; Westwood et al., in press) and has also been reported in numerous studies in the Arctic (Grossart et al., 2006; Allgaier et al., 2008; Paulino et al., 2008; Baragi et al., 2015; Wang et al., 2016), suggesting that the marine bacterial community will be resilient to increasing CO₂.

While we detected an increase in bacterial productivity, this response appeared to be correlated with an increase in Chl *a* concentration and available POM, rather than CO₂. Bacterial productivity was similar among all CO₂ treatments, except for a final promotion of productivity at 634 μatm on day 18 (Fig. 9b). This promotion of growth may be linked to an increase in diatom abundance observed in this treatment (Hancock et al., 2017). The coupling of bacterial growth with phytoplankton productivity has been reported by numerous studies on natural marine microbial communities (Allgaier et al., 2008; Grossart et al., 2006; Engel et al., 2013; Piontek et al., 2013; Sperling et al., 2013; Bergen et al., 2016). Thus, it is likely that the bacterial community was controlled more by grazing and nutrient availability than by CO₂ level.

5 Conclusions

These results support the identification of a tipping point in the marine microbial community response to CO₂ between 953 and 1140 μatm . When exposed to CO₂ $\geq 634 \mu\text{atm}$, declines in growth rates, primary productivity, and organic matter production were observed in the phytoplankton community and became significantly different when $\geq 1140 \mu\text{atm}$. Despite this, the community displayed the ability to adapt to these high CO₂ conditions, down-regulating CCMs and likely adjusting other intracellular mechanisms to cope with the added stress of low pH. However, the lag in growth and subsequent acclimation to high CO₂ conditions allowed for more tolerant species to thrive (Hancock et al., 2017).

Conditions in Antarctic coastal regions fluctuate throughout the seasons and the marine microbial community is already tolerant to changes in CO₂ level, light availability, and nutrients (Gibson and Trull, 1999; Roden et al., 2013). It is possible that phytoplankton communities already exposed to highly variable conditions will be more capable of adapting to the projected changes in CO₂ (Schaum and Collins, 2014; Boyd et al., 2016). Although, this will likely also include adaptation at the community level, causing a shift in dominance to more tolerant species. This has been observed in numerous ocean acidification

experiments, with a trend in community composition favouring picophytoplankton and away from large diatoms (Davidson et al., 2016; Reviewed in Schulz et al., 2017). Such a change in phytoplankton community composition may have flow on effects to higher trophic levels that feed on Antarctic phytoplankton blooms. It could also have a significant effect on the biological pump, with decreased carbon draw-down at high CO₂, causing a negative feedback on anthropogenic CO₂ uptake.

5 Coincident increases in bacterial abundance under high CO₂ conditions may also increase the efficiency of the microbial loop, resulting in increased organic matter remineralisation and further declines in carbon sequestration.

Data availability. Experimental data used for analysis are available via the Australian Antarctic Data Centre.

Environmental data: Deppeler, S.L., Davidson, A.T., Schulz, K.: Environmental data for Davis 14/15 ocean acidification minicosm experiment, Australian Antarctic Data Centre, <http://dx.doi.org/10.4225/15/599a7dfe9470a>, 2017, (updated 2017).

10 Productivity data: Deppeler, S.L., Petrou, K., Schulz, K., Davidson, A.T., Mckinlay, J., Pearce, I., Westwood, K.J.: Data for manuscript 'Ocean acidification of a coastal Antarctic marine microbial community reveals a critical threshold for CO₂ tolerance in phytoplankton productivity', Australian Antarctic Data Centre, <http://dx.doi.org/10.4225/15/599a7cc747c61>, 2017 (updated 2017).

15 *Author contributions.* AD, KW, and KP conceived and designed the experiments. AD led and oversaw the minicosm experiment. SD and KP performed the experiments and data analysis. KS performed the carbonate system measurements and manipulation. IP performed pigment extraction and analysis. JM provided statistical guidance. SD wrote the manuscript with significant input from KP, KS, and AD. All authors provided contributions and critical review of the manuscript.

Competing interests. The authors declare that they have no conflict of interest.

20 *Acknowledgements.* This study was funded by the Australian Government, Department of Environment and Energy as part of Australian Antarctic Science Project 4026 at the Australian Antarctic Division and an Elite Research Scholarship awarded by the Institute for Marine and Antarctic Studies, University of Tasmania. We would like to thank Prof. Andrew McMinn for valuable comments on our manuscript, Penelope Pascoe for the flow cytometric analyses, Cristin Sheehan for photosynthesis and respiration data, and Dr. Thomas Rodemann from the Central Science Laboratory, University of Tasmania for elemental analysis of our POM samples. We gratefully acknowledge the assistance of AAD technical support in designing and equipping the minicosms and Davis Station expeditioners in the summer of 2014/15 for their support and assistance.

References

Allgaier, M., Riebesell, U., Vogt, M., Thyrhaug, R., and Grossart, H.-P.: Coupling of heterotrophic bacteria to phytoplankton bloom development at different pCO₂ levels: a mesocosm study, *Biogeosciences*, 5, 1007–1022, doi:10.5194/bg-5-1007-2008, 2008.

Arrigo, K. R., van Dijken, G. L., and Bushinsky, S.: Primary production in the Southern Ocean, 1997–2006, *J. Geophys. Res. Ocean.*, 113, 5 C08 004, doi:10.1029/2007JC004551, 2008a.

Arrigo, K. R., van Dijken, G. L., and Long, M.: Coastal Southern Ocean: A strong anthropogenic CO₂ sink, *Geophys. Res. Lett.*, 35, L21 602, doi:10.1029/2008GL035624, 2008b.

Azam, F., Fenchel, T., Field, J. G., Gray, J. C., Meyer-Reil, L. A., and Thingstad, F.: The ecological role of water-column microbes in the sea, *Mar. Ecol. Prog. Ser.*, 10, 257–264, doi:10.3354/meps010257, 1983.

10 Azam, F., Smith, D. C., and Hollibaugh, J. T.: The role of the microbial loop in Antarctic pelagic ecosystems, *Polar Res.*, 10, 239–243, doi:10.1111/j.1751-8369.1991.tb00649.x, 1991.

Bach, L. T., Taucher, J., Boxhammer, T., Ludwig, A., Achterberg, E. P., Algueró-Muñiz, M., Anderson, L. G., Bellworthy, J., Büdenbender, J., Czerny, J., Ericson, Y., Esposito, M., Fischer, M., Haunost, M., Hellemann, D., Horn, H. G., Hornick, T., Meyer, J., Sswat, M., Zark, M., and Riebesell, U.: Influence of ocean acidification on a natural winter-to-summer plankton succession first insights from a long-term 15 mesocosm study draw attention to periods of low nutrient concentrations, *PLoS One*, 11, e0159 068, doi:10.1371/journal.pone.0159068, 2016.

Badger, M.: The Role of Carbonic Anhydrase in Photosynthesis, *Annu. Rev. Plant Physiol. Plant Mol. Biol.*, 45, 369–392, doi:10.1146/annurev.arplant.45.1.369, 1994.

Badger, M. R., Andrews, T. J., Whitney, S., Ludwig, M., Yellowlees, D. C., Leggat, W., and Price, G. D.: The diversity and coevolution of Ru-20 bisco, plastids, pyrenoids, and chloroplast-based CO₂-concentrating mechanisms in algae, *Can. J. Bot.*, 76, 1052–1071, doi:10.1139/cjb-76-6-1052, 1998.

Baragi, L. V., Khandeparker, L., and Anil, A. C.: Influence of elevated temperature and pCO₂ on the marine periphytic diatom *Navicula distans* and its associated organisms in culture, *Hydrobiologia*, 762, 127–142, doi:10.1007/s10750-015-2343-9, 2015.

Barcelos e Ramos, J., Schulz, K. G., Brownlee, C., Sett, S., and Azevedo, E. B.: Effects of Increasing Seawater Carbon Dioxide Concentra-25 tions on Chain Formation of the Diatom *Asterionellopsis glacialis*, *PLoS One*, 9, e90 749, doi:10.1371/journal.pone.0090749, 2014.

Behrenfeld, M. J., Prasil, O., Babin, M., and Bruyant, F.: In Search of a Physiological Basis for Covariations in Light-Limited and Light-Saturated Photosynthesis, *J. Phycol.*, 40, 4–25, doi:10.1046/j.1529-8817.2004.03083.x, 2004.

Behrenfeld, M. J., Halsey, K. H., and Milligan, A. J.: Evolved physiological responses of phytoplankton to their integrated growth environment., *Philos. Trans. R. Soc. B*, 363, 2687–2703, doi:10.1098/rstb.2008.0019, 2008.

30 Bellerby, R. G. J., Schulz, K. G., Riebesell, U., Neill, C., Nondal, G., Heegaard, E., Johannessen, T., and Brown, K. R.: Marine ecosystem community carbon and nutrient uptake stoichiometry under varying ocean acidification during the PeECE III experiment, *Biogeosciences*, 5, 1517–1527, doi:10.5194/bg-5-1517-2008, 2008.

Berge, T., Daugbjerg, N., Balling Andersen, B., and Hansen, P.: Effect of lowered pH on marine phytoplankton growth rates, *Mar. Ecol. Prog. Ser.*, 416, 79–91, doi:10.3354/meps08780, 2010.

35 Bergen, B., Endres, S., Engel, A., Zark, M., Dittmar, T., Sommer, U., and Jürgens, K.: Acidification and warming affect prominent bacteria in two seasonal phytoplankton bloom mesocosms, *Environ. Microbiol.*, 18, 4579–4595, doi:10.1111/1462-2920.13549, 2016.

Bi, R., Ismar, S., Sommer, U., and Zhao, M.: Environmental dependence of the correlations between stoichiometric and fatty acid-based indicators of phytoplankton nutritional quality, *Limnol. Oceanogr.*, 62, 334–347, doi:10.1002/lo.10429, 2017.

Bockmon, E. E. and Dickson, A. G.: A seawater filtration method suitable for total dissolved inorganic carbon and pH analyses, *Limnol. Oceanogr. Methods*, 12, 191–195, doi:10.4319/lom.2014.12.191, 2014.

5 Boyd, P. W., Doney, S. C., Strzepek, R., Dusenberry, J., Lindsay, K., and Fung, I.: Climate-mediated changes to mixed-layer properties in the Southern Ocean: assessing the phytoplankton response, *Biogeosciences*, 5, 847–864, doi:10.5194/bg-5-847-2008, 2008.

Boyd, P. W., Cornwall, C. E., Davidson, A., Doney, S. C., Fourquez, M., Hurd, C. L., Lima, I. D., and McMinn, A.: Biological responses to environmental heterogeneity under future ocean conditions, *Glob. Chang. Biol.*, 22, 2633–2650, doi:10.1111/gcb.13287, 2016.

Bunse, C., Lundin, D., Karlsson, C. M. G., Vila-Costa, M., Palovaara, J., Akram, N., Svensson, L., Holmfeldt, K., González, J. M., Calvo, 10 Pelejero, C., Marrasé, C., Dopson, M., Gasol, J. M., and Pinhassi, J.: Response of marine bacterioplankton pH homeostasis gene expression to elevated CO₂, *Nat. Clim. Chang.*, 1, 1–7, doi:10.1038/nclimate2914, 2016.

Burkhardt, S., Amoroso, G., Riebesell, U., and Sültemeyer, D.: CO₂ and HCO₃[−] uptake in marine diatoms acclimated to different CO₂ concentrations, *Limnol. Oceanogr.*, 46, 1378–1391, doi:10.4319/lo.2001.46.6.1378, 2001.

Caldeira, K. and Wickett, M. E.: Oceanography: Anthropogenic carbon and ocean pH, *Nature*, 425, 365–365, doi:10.1038/425365a, 2003.

15 Cassar, N., Laws, E. A., Bidigare, R. R., and Popp, B. N.: Bicarbonate uptake by Southern Ocean phytoplankton, *Global Biogeochem. Cycles*, 18, 1–10, doi:10.1029/2003GB002116, 2004.

Chen, C. and Durbin, E.: Effects of pH on the growth and carbon uptake of marine phytoplankton, *Mar. Ecol. Prog. Ser.*, 109, 83–94, doi:10.3354/meps109083, 1994.

Chen, H., Guan, W., Zeng, G., Li, P., and Chen, S.: Alleviation of solar ultraviolet radiation (UVR)-induced photoinhibition in diatom 20 *Chaetoceros curvisetus* by ocean acidification, *J. Mar. Biol. Assoc. United Kingdom*, 95, 661–667, doi:10.1017/S0025315414001568, 2015.

Coad, T., McMinn, A., Nomura, D., and Martin, A.: Effect of elevated CO₂ concentration on microalgal communities in Antarctic pack ice, *Deep Sea Res. Part II Top. Stud. Oceanogr.*, 131, 160–169, doi:10.1016/j.dsr2.2016.01.005, 2016.

25 Davidson, A., McKinlay, J., Westwood, K., Thomson, P., van den Enden, R., de Salas, M., Wright, S., Johnson, R., and Berry, K.: Enhanced CO₂ concentrations change the structure of Antarctic marine microbial communities, *Mar. Ecol. Prog. Ser.*, 552, 93–113, doi:10.3354/meps11742, 2016.

Deppeler, S. L. and Davidson, A. T.: Southern Ocean Phytoplankton in a Changing Climate, *Front. Mar. Sci.*, 4, 40, doi:10.3389/fmars.2017.00040, 2017.

Dickson, A.: Standards for Ocean Measurements, *Oceanography*, 23, 34–47, doi:10.5670/oceanog.2010.22, 2010.

30 Dickson, A., Sabine, C., and Christian, J., eds.: Guide to Best Practices for Ocean CO₂ Measurements, North Pacific Marine Science Organization, Sidney, British Columbia, 2007.

Dring, M. J. and Jewson, D. H.: What Does 14C Uptake by Phytoplankton Really Measure? A Theoretical Modelling Approach, *Proc. R. Soc. B Biol. Sci.*, 214, 351–368, doi:10.1098/rspb.1982.0016, 1982.

Ducklow, H. W., Baker, K., Martinson, D. G., Quetin, L. B., Ross, R. M., Smith, R. C., Stammerjohn, S. E., Vernet, M., and Fraser, W.: 35 Marine pelagic ecosystems: the West Antarctic Peninsula, *Philos. Trans. R. Soc. B Biol. Sci.*, 362, 67–94, doi:10.1098/rstb.2006.1955, 2007.

Egge, J. K., Thingstad, T. F., Larsen, A., Engel, A., Wohlers, J., Bellerby, R. G. J., and Riebesell, U.: Primary production during nutrient-induced blooms at elevated CO₂ concentrations, *Biogeosciences*, 6, 877–885, doi:10.5194/bg-6-877-2009, 2009.

Engel, A., Borchard, C., Piontek, J., Schulz, K. G., Riebesell, U., and Bellerby, R.: CO₂ increases ¹⁴C primary production in an Arctic plankton community, *Biogeosciences*, 10, 1291–1308, doi:10.5194/bg-10-1291-2013, 2013.

Engel, A., Piontek, J., Grossart, H.-P., Riebesell, U., Schulz, K. G., and Sperling, M.: Impact of CO₂ enrichment on organic matter dynamics during nutrient induced coastal phytoplankton blooms, *J. Plankton Res.*, 36, 641–657, doi:10.1093/plankt/fbt125, 2014.

5 Fabry, V., McClintock, J., Mathis, J., and Grebmeier, J.: Ocean Acidification at High Latitudes: The Bellwether, *Oceanography*, 22, 160–171, doi:10.5670/oceanog.2009.105, 2009.

Fenchel, T.: The microbial loop - 25 years later, *J. Exp. Mar. Bio. Ecol.*, 366, 99–103, doi:10.1016/j.jembe.2008.07.013, 2008.

Feng, Y., Hare, C., Rose, J., Handy, S., DiTullio, G., Lee, P., Smith, W. J., Peloquin, J., Tozzi, S., Sun, J., Zhang, Y., Dunbar, R., Long, M., Sohst, B., Lohan, M., and Hutchins, D.: Interactive effects of iron, irradiance and CO₂ on Ross Sea phytoplankton, *Deep Sea Res. Part I Oceanogr. Res. Pap.*, 57, 368–383, doi:10.1016/j.dsr.2009.10.013, 2010.

10 Finkel, Z. V., Beardall, J., Flynn, K. J., Quigg, A., Rees, T. A. V., and Raven, J. A.: Phytoplankton in a changing world: cell size and elemental stoichiometry, *J. Plankton Res.*, 32, 119–137, doi:10.1093/plankt/fbp098, 2010.

Frölicher, T. L., Sarmiento, J. L., Paynter, D. J., Dunne, J. P., Krasting, J. P., and Winton, M.: Dominance of the Southern Ocean in Anthropogenic Carbon and Heat Uptake in CMIP5 Models, *J. Clim.*, 28, 862–886, doi:10.1175/JCLI-D-14-00117.1, 2015.

15 Gao, K. and Campbell, D. A.: Photophysiological responses of marine diatoms to elevated CO₂ and decreased pH: a review, *Funct. Plant Biol.*, 41, 449–459, doi:10.1071/FP13247, 2014.

Gao, K., Helbling, E., Häder, D., and Hutchins, D.: Responses of marine primary producers to interactions between ocean acidification, solar radiation, and warming, *Mar. Ecol. Prog. Ser.*, 470, 167–189, doi:10.3354/meps10043, 2012a.

Gao, K., Xu, J., Gao, G., Li, Y., Hutchins, D. A., Huang, B., Wang, L., Zheng, Y., Jin, P., Cai, X., Häder, D.-p., Li, W., Xu, K., Liu, N., 20 and Riebesell, U.: Rising CO₂ and increased light exposure synergistically reduce marine primary productivity, *Nat. Clim. Chang.*, 2, 519–523, doi:10.1038/nclimate1507, 2012b.

Gattuso, J.-P., Gao, K., Lee, K., Rost, B., and Schulz, K. G.: Approaches and tools to manipulate the carbonate chemistry, in: Guide to best practices for ocean acidification research and data reporting, edited by Riebesell, U., Fabry, V. J., Hansson, L., and Gattuso, J.-P., chap. 2, pp. 41–52, Publications Office of the European Union, Luxembourg, doi:10.2777/66906, 2010.

25 Gibson, J. A. and Trull, T. W.: Annual cycle of *f*CO₂ under sea-ice and in open water in Prydz Bay, East Antarctica, *Mar. Chem.*, 66, 187–200, doi:10.1016/S0304-4203(99)00040-7, 1999.

González, N., Gattuso, J. P., and Middelburg, J. J.: Oxygen production and carbon fixation in oligotrophic coastal bays and the relationship with gross and net primary production, *Aquat. Microb. Ecol.*, 52, 119–130, doi:10.3354/ame01208, 2008.

Grossart, H.-P., Allgaier, M., Passow, U., and Riebesell, U.: Testing the effect of CO₂ concentration on the dynamics of marine heterotrophic 30 bacterioplankton, *Limnol. Oceanogr.*, 51, 1–11, doi:10.4319/lo.2006.51.1.0001, 2006.

Halsey, K. H., Milligan, A. J., and Behrenfeld, M. J.: Physiological optimization underlies growth rate-independent chlorophyll-specific gross and net primary production, *Photosynth. Res.*, 103, 125–137, doi:10.1007/s11120-009-9526-z, 2010.

Hancock, A. M., Davidson, A. T., McKinlay, J., McMinn, A., Schulz, K., and van den Enden, R. L.: Ocean acidification changes the structure of an Antarctic coastal protistan community, *Biogeosciences Discuss.*, in review, 1–32, doi:10.5194/bg-2017-224, 2017.

35 Hauck, J. and Völker, C.: Rising atmospheric CO₂ leads to large impact of biology on Southern Ocean CO₂ uptake via changes of the Revelle factor, *Geophys. Res. Lett.*, 42, 1459–1464, doi:10.1002/2015GL063070, 2015.

Hauck, J., Völker, C., Wolf-Gladrow, D. A., Laufkötter, C., Vogt, M., Aumont, O., Bopp, L., Buitenhuis, E. T., Doney, S. C., Dunne, J., Gruber, N., Hashioka, T., John, J., Quéré, C. L., Lima, I. D., Nakano, H., Séférian, R., and Totterdell, I.: On the Southern Ocean CO₂ uptake and

the role of the biological carbon pump in the 21st century, *Global Biogeochem. Cycles*, 29, 1451–1470, doi:10.1002/2015GB005140, 2015.

Hennon, G. M. M., Quay, P., Morales, R. L., Swanson, L. M., and Virginia Armbrust, E.: Acclimation conditions modify physiological response of the diatom *Thalassiosira pseudonana* to elevated CO₂ concentrations in a nitrate-limited chemostat, *J. Phycol.*, 50, 243–253, 5 doi:10.1111/jpy.12156, 2014.

Hennon, G. M. M., Ashworth, J., Groussman, R. D., Berthiaume, C., Morales, R. L., Baliga, N. S., Orellana, M. V., and Armbrust, E. V.: Diatom acclimation to elevated CO₂ via cAMP signalling and coordinated gene expression, *Nat. Clim. Chang.*, 5, 761–765, doi:10.1038/nclimate2683, 2015.

Holding, J. M., Duarte, C. M., Sanz-Martín, M., Mesa, E., Arrieta, J. M., Chierici, M., Hendriks, I. E., García-Corral, L. S., Regaudie-de 10 Gioux, A., Delgado, A., Reigstad, M., Wassmann, P., and Agustí, S.: Temperature dependence of CO₂-enhanced primary production in the European Arctic Ocean, *Nat. Clim. Chang.*, 5, 1079–1082, doi:10.1038/nclimate2768, 2015.

Hong, H., Li, D., Lin, W., Li, W., and Shi, D.: Nitrogen nutritional condition affects the response of energy metabolism in diatoms to elevated carbon dioxide, *Mar. Ecol. Prog. Ser.*, 567, 41–56, doi:10.3354/meps12033, 2017.

Honjo, S.: Particle export and the biological pump in the Southern Ocean, *Antarct. Sci.*, 16, 501–516, doi:10.1017/S0954102004002287, 15 2004.

Hopkinson, B. M., Xu, Y., Shi, D., McGinn, P. J., and Morel, F. M. M.: The effect of CO₂ on the photosynthetic physiology of phytoplankton in the Gulf of Alaska, *Limnol. Oceanogr.*, 55, 2011–2024, doi:10.4319/lo.2010.55.5.2011, 2010.

Hopkinson, B. M., Dupont, C. L., Allen, A. E., and Morel, F. M. M.: Efficiency of the CO₂-concentrating mechanism of diatoms, *Proc. Natl. Acad. Sci.*, 108, 3830–3837, doi:10.1073/pnas.1018062108, 2011.

Hoppe, C. J. M., Hassler, C. S., Payne, C. D., Tortell, P. D., Rost, B., and Trimborn, S.: Iron Limitation Modulates Ocean Acidification 20 Effects on Southern Ocean Phytoplankton Communities, *PLoS One*, 8, e79 890, doi:10.1371/journal.pone.0079890, 2013.

Hoppe, C. J. M., Holtz, L.-M., Trimborn, S., and Rost, B.: Ocean acidification decreases the light-use efficiency in an Antarctic diatom under dynamic but not constant light, *New Phytol.*, 207, 159–171, doi:10.1111/nph.13334, 2015.

Hoppema, M., Fahrbach, E., Schröder, M., Wisotzki, A., and de Baar, H. J.: Winter-summer differences of carbon dioxide and oxygen in the 25 Weddell Sea surface layer, *Mar. Chem.*, 51, 177–192, doi:10.1016/0304-4203(95)00065-8, 1995.

IPCC: Climate Change 2013: The Physical Science Basis. Contribution of Working Group I to the Fifth Assessment Report of the Intergovernmental Panel on Climate Change, Cambridge University Press, Cambridge, United Kingdom and New York, NY, USA, doi:10.1017/CBO9781107415324, 2013.

Jeffrey, S. and Humphrey, G.: New spectrophotometric equations for determining chlorophylls *a*, *b*, *c₁* and *c₂* in higher plants, algae and 30 natural phytoplankton, *Biochem. und Physiol. der Pflanz.*, 167, 191–194, doi:10.1016/S0015-3796(17)30778-3, 1975.

Jeffrey, S. W. and Wright, S. W.: Qualitative and quantitative HPLC analysis of SCOR reference algal cultures, in: *Phytoplankton Pigments in Oceanography: Guidelines to Modern Methods*, edited by Jeffrey, S., Mantoura, R., and Wright, S., pp. 343–360, UNESCO, Paris, 1997.

Kähler, P. and Koeve, W.: Marine dissolved organic matter: Can its C:N ratio explain carbon overconsumption?, *Deep. Res. Part I Oceanogr. Res. Pap.*, 48, 49–62, doi:10.1016/S0967-0637(00)00034-0, 2001.

Khatiwala, S., Primeau, F., and Hall, T.: Reconstruction of the history of anthropogenic CO₂ concentrations in the ocean, *Nature*, 462, 346–349, doi:10.1038/nature08526, 2009.

Kim, J.-M., Lee, K., Shin, K., Kang, J.-H., Lee, H.-W., Kim, M., Jang, P.-G., and Jang, M.-C.: The effect of seawater CO₂ concentration on growth of a natural phytoplankton assemblage in a controlled mesocosm experiment, *Limnol. Oceanogr.*, 51, 1629–1636, doi:10.4319/lo.2006.51.4.1629, 2006.

King, A., Jenkins, B., Wallace, J., Liu, Y., Wikfors, G., Milke, L., and Meseck, S.: Effects of CO₂ on growth rate, C:N:P, and fatty acid composition of seven marine phytoplankton species, *Mar. Ecol. Prog. Ser.*, 537, 59–69, doi:10.3354/meps11458, 2015.

5 Kirchman, D. L.: Measuring Bacterial Biomass Production and Growth Rates from Leucine Incorporation in Natural Aquatic Environments, in: *Methods in Microbiology*, edited by Paul, J., vol. 30, chap. 12, pp. 227–237, Academic Press, St Petersburg, FL, doi:10.1016/S0580-9517(01)30047-8, 2001.

Kirchman, D. L.: *Microbial ecology of the oceans*, Wiley-Blackwell, Hoboken, N.J., 2 edn., 2008.

10 Legendre, L., Ackley, S. F., Dieckmann, G. S., Gulliksen, B., Horner, R., Hoshiai, T., Melnikov, I. A., Reeburgh, W. S., Spindler, M., and Sullivan, C. W.: Ecology of sea ice biota - 2. Global significance, *Polar Biol.*, 12, 429–444, doi:10.1007/BF00243114, 1992.

Lewis, M. and Smith, J.: A small volume, short-incubation-time method for measurement of photosynthesis as a function of incident irradiance, *Mar. Ecol. Prog. Ser.*, 13, 99–102, doi:10.3354/meps013099, 1983.

15 Li, F., Beardall, J., Collins, S., and Gao, K.: Decreased photosynthesis and growth with reduced respiration in the model diatom *Phaeodactylum tricornutum* grown under elevated CO₂ over 1800 generations, *Glob. Chang. Biol.*, 23, 127–137, doi:10.1111/gcb.13501, 2017a.

Li, W., Yang, Y., Li, Z., Xu, J., and Gao, K.: Effects of seawater acidification on the growth rates of the diatom *Thalassiosira (Conticribra) weissflogii* under different nutrient, light, and UV radiation regimes, *J. Appl. Phycol.*, 29, 133–142, doi:10.1007/s10811-016-0944-y, 2017b.

Liu, N., Beardall, J., and Gao, K.: Elevated CO₂ and associated seawater chemistry do not benefit a model diatom grown with increased 20 availability of light, *Aquat. Microb. Ecol.*, 79, 137–147, doi:10.3354/ame01820, 2017.

Longhurst, A. R.: Role of the marine biosphere in the global carbon cycle, *Limnol. Oceanogr.*, 36, 1507–1526, doi:10.4319/lo.1991.36.8.1507, 1991.

25 Lueker, T. J., Dickson, A. G., and Keeling, C. D.: Ocean pCO₂ calculated from dissolved inorganic carbon, alkalinity, and equations for K₁ and K₂: validation based on laboratory measurements of CO₂ in gas and seawater at equilibrium, *Mar. Chem.*, 70, 105–119, doi:10.1016/S0304-4203(00)00022-0, 2000.

Mantoura, R. and Repeta, D.: Calibration methods for HPLC, in: *Phytoplankton Pigments in Oceanography: Guidelines to Modern Methods*, edited by Jeffrey, S., Mantoura, R., and Wright, S., pp. 407–428, UNESCO, Paris, 1997.

Marie, D., Simon, N., and Vaulot, D.: Phytoplankton cell counting by flow cytometry, in: *Algal Culturing Techniques*, edited by Anderson, R. A., chap. 17, pp. 253–267, Academic Press, San Diego, CA, USA, doi:10.1016/B978-012088426-1/50018-4, 2005.

30 McMinn, A., Müller, M. N., Martin, A., and Ryan, K. G.: The Response of Antarctic Sea Ice Algae to Changes in pH and CO₂, *PLoS One*, 9, e86984, doi:10.1371/journal.pone.0086984, 2014.

McNeil, B. I. and Matear, R. J.: Southern Ocean acidification: A tipping point at 450-ppm atmospheric CO₂, *Proc. Natl. Acad. Sci.*, 105, 18 860–18 864, doi:10.1073/pnas.0806318105, 2008.

Mehrbach, C., Culberson, C. H., Hawley, J. E., and Pytkowicz, R. M.: Measurement of the Apparent Dissociation Constants of Carbonic 35 Acid in Seawater At Atmospheric Pressure, *Limnol. Oceanogr.*, 18, 897–907, doi:10.4319/lo.1973.18.6.0897, 1973.

Meinshausen, M., Smith, S. J., Calvin, K., Daniel, J. S., Kainuma, M. L. T., Lamarque, J., Matsumoto, K., Montzka, S. A., Raper, S. C. B., Riahi, K., Thomson, A., Velders, G. J. M., and van Vuuren, D. P. P.: The RCP greenhouse gas concentrations and their extensions from 1765 to 2300, *Clim. Change*, 109, 213–241, doi:10.1007/s10584-011-0156-z, 2011.

Metzl, N., Tilbrook, B., and Poisson, A.: The annual $f\text{CO}_2$ cycle and the air-sea CO_2 flux in the sub-Antarctic Ocean, *Tellus B*, 51, 849–861, doi:10.1034/j.1600-0889.1999.t01-3-00008.x, 1999.

Moreau, S., Schloss, I., Mostajir, B., Demers, S., Almundoz, G., Ferrario, M., and Ferreyra, G.: Influence of microbial community composition and metabolism on air-sea ΔpCO_2 variation off the western Antarctic Peninsula, *Mar. Ecol. Prog. Ser.*, 446, 45–59, doi:10.3354/meps09466, 2012.

Nelson, D. M., Smith, W. O. J., Gordon, L. I., and Huber, B. A.: Spring distributions of density, nutrients, and phytoplankton biomass in the ice edge zone of the Weddell-Scotia Sea, *J. Geophys. Res. Ocean.*, 92, 7181, doi:10.1029/JC092iC07p07181, 1987.

Orr, J. C., Fabry, V. J., Aumont, O., Bopp, L., Doney, S. C., Feely, R. A., Gnanadesikan, A., Gruber, N., Ishida, A., Joos, F., Key, R. M., Lindsay, K., Maier-Reimer, E., Matear, R., Monfray, P., Mouchet, A., Najjar, R. G., Plattner, G.-K., Rodgers, K. B., Sabine, C. L., Sarmiento, J. L., Schlitzer, R., Slater, R. D., Totterdell, I. J., Weirig, M.-F., Yamanaka, Y., and Yool, A.: Anthropogenic ocean acidification over the twenty-first century and its impact on calcifying organisms, *Nature*, 437, 681–6, doi:10.1038/nature04095, 2005.

Pasquer, B., Mongin, M., Johnston, N., and Wright, S.: Distribution of particulate organic matter (POM) in the Southern Ocean during BROKE-West (30°E - 80°E), *Deep Sea Res. Part II Top. Stud. Oceanogr.*, 57, 779–793, doi:10.1016/j.dsr2.2008.12.040, 2010.

Paul, C., Matthiessen, B., and Sommer, U.: Warming, but not enhanced CO_2 concentration, quantitatively and qualitatively affects phytoplankton biomass, *Mar. Ecol. Prog. Ser.*, 528, 39–51, doi:10.3354/meps11264, 2015.

Paulino, A. I., Egge, J. K., and Larsen, A.: Effects of increased atmospheric CO_2 on small and intermediate sized osmotrophs during a nutrient induced phytoplankton bloom, *Biogeosciences*, 5, 739–748, doi:10.5194/bg-5-739-2008, 2008.

Pearce, I., Davidson, A., Bell, E., and Wright, S.: Seasonal changes in the concentration and metabolic activity of bacteria and viruses at an Antarctic coastal site, *Aquat. Microb. Ecol.*, 47, 11–23, doi:10.3354/ame047011, 2007.

Pearce, I., Davidson, A. T., Thomson, P. G., Wright, S., and van den Enden, R.: Marine microbial ecology off East Antarctica (30 - 80°E): Rates of bacterial and phytoplankton growth and grazing by heterotrophic protists, *Deep Sea Res. Part II Top. Stud. Oceanogr.*, 57, 849–862, doi:10.1016/j.dsr2.2008.04.039, 2010.

Perrin, R. A., Lu, P., and Marchant, H. J.: Seasonal variation in marine phytoplankton and ice algae at a shallow Antarctic coastal site, *Hydrobiologia*, 146, 33–46, doi:10.1007/BF00007575, 1987.

Petrou, K., Kranz, S. A., Trimborn, S., Hassler, C. S., Ameijeiras, S. B., Sackett, O., Ralph, P. J., and Davidson, A. T.: Southern Ocean phytoplankton physiology in a changing climate, *J. Plant Physiol.*, 203, 135–150, doi:10.1016/j.jplph.2016.05.004, 2016.

Piontek, J., Borchard, C., Sperling, M., Schulz, K. G., Riebesell, U., and Engel, A.: Response of bacterioplankton activity in an Arctic fjord system to elevated pCO_2 : results from a mesocosm perturbation study, *Biogeosciences*, 10, 297–314, doi:10.5194/bg-10-297-2013, 2013.

Platt, T., Gallegos, C. L., and Harrison, W. G.: Photoinhibition of photosynthesis in natural assemblages of marine phytoplankton, *J. Mar. Res.*, 38, 687–701, 1980.

Polimene, L., Sailley, S., Clark, D., Mitra, A., and Allen, J. I.: Biological or microbial carbon pump? The role of phytoplankton stoichiometry in ocean carbon sequestration, *J. Plankton Res.*, 39, 180–186, doi:10.1093/plankt/fbw091, 2016.

R Core Team: R: A Language and Environment for Statistical Computing, R Foundation for Statistical Computing, Vienna, Austria, <https://www.R-project.org/>, 2016.

Raven, J. A.: Physiology of inorganic C acquisition and implications for resource use efficiency by marine phytoplankton: relation to increased CO_2 and temperature, *Plant, Cell Environ.*, 14, 779–794, doi:10.1111/j.1365-3040.1991.tb01442.x, 1991.

Raven, J. A. and Falkowski, P. G.: Oceanic sinks for atmospheric CO_2 , *Plant, Cell Environ.*, 22, 741–755, doi:10.1046/j.1365-3040.1999.00419.x, 1999.

Raven, J. A., Caldeira, K., Elderfield, H., Hoegh-Guldberg, O., Liss, P., Riebesell, U., Shepherd, J., Turley, C., and Watson, A.: Ocean acidification due to increasing atmospheric carbon dioxide, Tech. Rep. June, The Royal Society, 2005.

Regaudie-de Gioux, A., Lasternas, S., Agustí, S., Duarte, C. M., and Benítez, N. G.: Comparing marine primary production estimates through different methods and development of conversion equations, *Front. Mar. Sci.*, 1, 1–14, doi:10.3389/fmars.2014.00019, 2014.

5 Riebesell, U.: Effects of CO₂ Enrichment on Marine Phytoplankton, *J. Oceanogr.*, 60, 719–729, doi:10.1007/s10872-004-5764-z, 2004.

Riebesell, U., Schulz, K. G., Bellerby, R. G. J., Botros, M., Fritsche, P., Meyerhöfer, M., Neill, C., Nondal, G., Oschlies, A., Wohlers, J., and Zöllner, E.: Enhanced biological carbon consumption in a high CO₂ ocean, *Nature*, 450, 545–548, doi:10.1038/nature06267, 2007.

Riebesell, U., Gattuso, J.-P., Thingstad, T. F., and Middelburg, J. J.: Preface "Arctic ocean acidification: pelagic ecosystem and biogeochemical responses during a mesocosm study", *Biogeosciences*, 10, 5619–5626, doi:10.5194/bg-10-5619-2013, 2013.

10 Riley, G. A.: Phytoplankton of the North Central Sargasso Sea, 1950–521, *Limnol. Oceanogr.*, 2, 252–270, doi:10.1002/lno.1957.2.3.0252, 1957.

Ritchie, R. J.: Consistent sets of spectrophotometric chlorophyll equations for acetone, methanol and ethanol solvents, *Photosynth. Res.*, 89, 27–41, doi:10.1007/s11120-006-9065-9, 2006.

Roden, N. P., Shadwick, E. H., Tilbrook, B., and Trull, T. W.: Annual cycle of carbonate chemistry and decadal change in coastal Prydz Bay, 15 East Antarctica, *Mar. Chem.*, 155, 135–147, doi:10.1016/j.marchem.2013.06.006, 2013.

Rost, B., Riebesell, U., Burkhardt, S., and Sültemeyer, D.: Carbon acquisition of bloom-forming marine phytoplankton, *Limnol. Oceanogr.*, 48, 55–67, doi:10.4319/lo.2003.48.1.0055, 2003.

Sabine, C. L., Feely, R. A., Gruber, N., Key, R. M., Lee, K., Bullister, J. L., Wanninkhof, R., Wong, C. S., Wallace, D. W. R., Tilbrook, B., Millero, F. J., Peng, T.-H., Kozyr, A., Ono, T., and Rios, A. F.: The Oceanic Sink for Anthropogenic CO₂, *Science*, 305, 367–371, 20, doi:10.1126/science.1097403, 2004.

Satoh, A., Kurano, N., and Miyachi, S.: Inhibition of photosynthesis by intracellular carbonic anhydrase in microalgae under excess concentrations of CO₂, *Photosynth. Res.*, 68, 215–224, doi:10.1023/A:1012980223847, 2001.

Schaum, C. E. and Collins, S.: Plasticity predicts evolution in a marine alga, *Proc. R. Soc. B Biol. Sci.*, 281, 20141486–20141486, doi:10.1098/rspb.2014.1486, 2014.

25 Schaum, E., Rost, B., Millar, A. J., and Collins, S.: Variation in plastic responses of a globally distributed picoplankton species to ocean acidification, *Nat. Clim. Chang.*, 3, 298–302, doi:10.1038/nclimate1774, 2012.

Schreiber, U.: Pulse-Amplitude-Modulation (PAM) Fluorometry and Saturation Pulse Method: An Overview, in: *Chlorophyll a Fluorescence*, edited by Papageorgiou, G. C. and Govindjee, pp. 279–319, Springer Netherlands, Dordrecht, doi:10.1007/978-1-4020-3218-9_11, 2004.

Schulz, K. G., Bellerby, R. G. J., Brussaard, C. P. D., Büdenbender, J., Czerny, J., Engel, A., Fischer, M., Koch-Klavsen, S., Krug, S. A., 30 Lischka, S., Ludwig, A., Meyerhöfer, M., Nondal, G., Silyakova, A., Stuhr, A., and Riebesell, U.: Temporal biomass dynamics of an Arctic plankton bloom in response to increasing levels of atmospheric carbon dioxide, *Biogeosciences*, 10, 161–180, doi:10.5194/bg-10-161-2013, 2013.

Schulz, K. G., Bach, L. T., Bellerby, R. G. J., Bermúdez, R., Büdenbender, J., Boxhammer, T., Czerny, J., Engel, A., Ludwig, A., Meyerhöfer, M., Larsen, A., Paul, A. J., Sswat, M., and Riebesell, U.: Phytoplankton Blooms at Increasing Levels of Atmospheric Carbon Dioxide: Experimental Evidence for Negative Effects on Prymnesiophytes and Positive on Small Picoplankton, *Front. Mar. Sci.*, 4, 64, doi:10.3389/fmars.2017.00064, 2017.

35 Shi, D., Xu, Y., and Morel, F. M. M.: Effects of the pH/pCO₂ control method on medium chemistry and phytoplankton growth, *Biogeosciences*, 6, 1199–1207, doi:10.5194/bg-6-1199-2009, 2009.

Shi, Q., Xiahou, W., and Wu, H.: Photosynthetic responses of the marine diatom *Thalassiosira pseudonana* to CO₂-induced seawater acidification, *Hydrobiologia*, 788, 361–369, doi:10.1007/s10750-016-3014-1, 2017.

Silsbe, G. M. and Malkin, S. Y.: phytotools: Phytoplankton Production Tools, <https://CRAN.R-project.org/package=phytotoools>, R package version 1.0, 2015.

5 Simon, M. and Azam, F.: Protein content and protein synthesis rates of planktonic marine bacteria, *Mar. Ecol. Prog. Ser.*, 51, 201–213, doi:10.3354/meps051201, 1989.

Smith, W. O. and Nelson, D. M.: Importance of Ice Edge Phytoplankton Production in the Southern Ocean, *Bioscience*, 36, 251–257, doi:10.2307/1310215, 1986.

Sobrino, C., Ward, M. L., and Neale, P. J.: Acclimation to elevated carbon dioxide and ultraviolet radiation in the diatom *Thalassiosira pseudonana*: Effects on growth, photosynthesis, and spectral sensitivity of photoinhibition, *Limnol. Oceanogr.*, 53, 494–505, doi:10.4319/lo.2008.53.2.0494, 2008.

10 Sommer, U., Paul, C., and Moustaka-Gouni, M.: Warming and Ocean Acidification Effects on Phytoplankton—From Species Shifts to Size Shifts within Species in a Mesocosm Experiment, *PLoS One*, 10, e0125239, doi:10.1371/journal.pone.0125239, 2015.

Sperling, M., Piontek, J., Gerdts, G., Wichels, A., Schunck, H., Roy, A.-S., La Roche, J., Gilbert, J., Nissimov, J. I., Bittner, L., Romac, S.,
15 Riebesell, U., and Engel, A.: Effect of elevated CO₂ on the dynamics of particle-attached and free-living bacterioplankton communities in an Arctic fjord, *Biogeosciences*, 10, 181–191, doi:10.5194/bg-10-181-2013, 2013.

Spilling, K., Paul, A. J., Virkkala, N., Hastings, T., Lischka, S., Stuhr, A., Bermúdez, R., Czerny, J., Boxhammer, T., Schulz, K. G., Ludwig, A., and Riebesell, U.: Ocean acidification decreases plankton respiration: evidence from a mesocosm experiment, *Biogeosciences*, 13, 4707–4719, doi:10.5194/bg-13-4707-2016, 2016.

20 Steemann Nielsen, E.: The Use of Radio-active Carbon (C¹⁴) for Measuring Organic Production in the Sea, *ICES J. Mar. Sci.*, 18, 117–140, doi:10.1093/icesjms/18.2.117, 1952.

Takahashi, T., Sutherland, S. C., Wanninkhof, R., Sweeney, C., Feely, R. A., Chipman, D. W., Hales, B., Friederich, G., Chavez, F., Sabine, C., Watson, A., Bakker, D. C., Schuster, U., Metzl, N., Yoshikawa-Inoue, H., Ishii, M., Midorikawa, T., Nojiri, Y., Körtzinger, A., Steinhoff, T., Hoppema, M., Olafsson, J., Arnarson, T. S., Tilbrook, B., Johannessen, T., Olsen, A., Bellerby, R., Wong, C., Delille, B., Bates, N., and
25 de Baar, H. J.: Climatological mean and decadal change in surface ocean pCO₂, and net sea–air CO₂ flux over the global oceans, *Deep Sea Res. Part II Top. Stud. Oceanogr.*, 56, 554–577, doi:10.1016/j.dsr2.2008.12.009, 2009.

Takahashi, T., Sweeney, C., Hales, B., Chipman, D., Newberger, T., Goddard, J., Iannuzzi, R., and Sutherland, S.: The Changing Carbon Cycle in the Southern Ocean, *Oceanography*, 25, 26–37, doi:10.5670/oceanog.2012.71, 2012.

Tanaka, T., Alliouane, S., Bellerby, R. G. B., Czerny, J., de Kluijver, A., Riebesell, U., Schulz, K. G., Silyakova, A., and Gattuso, J.-P.: Effect
30 of increased pCO₂ on the planktonic metabolic balance during a mesocosm experiment in an Arctic fjord, *Biogeosciences*, 10, 315–325, doi:10.5194/bg-10-315-2013, 2013.

Taylor, A. R., Brownlee, C., and Wheeler, G. L.: Proton channels in algae: reasons to be excited, *Trends Plant Sci.*, 17, 675–684, doi:10.1016/j.tplants.2012.06.009, 2012.

Tew, K. S., Kao, Y.-C., Ko, F.-C., Kuo, J., Meng, P.-J., Liu, P.-J., and Glover, D. C.: Effects of elevated CO₂ and temperature on the growth, elemental composition, and cell size of two marine diatoms: potential implications of global climate change, *Hydrobiologia*, 741, 79–87, doi:10.1007/s10750-014-1856-y, 2014.

35 Thomson, P., Davidson, A., and Maher, L.: Increasing CO₂ changes community composition of pico- and nano-sized protists and prokaryotes at a coastal Antarctic site, *Mar. Ecol. Prog. Ser.*, 554, 51–69, doi:10.3354/meps11803, 2016.

Torstensson, A., Hedblom, M., Mattsdotter Björk, M., Chierici, M., and Wulff, A.: Long-term acclimation to elevated pCO₂ alters carbon metabolism and reduces growth in the Antarctic diatom *Nitzschia lecointei*, Proc. R. Soc. B Biol. Sci., 282, 20151513, doi:10.1098/rspb.2015.1513, 2015.

Tortell, P. D. and Morel, F. M. M.: Sources of inorganic carbon for phytoplankton in the eastern Subtropical and Equatorial Pacific Ocean, 5 Limnol. Oceanogr., 47, 1012–1022, doi:10.4319/lo.2002.47.4.1012, 2002.

Tortell, P. D., Rau, G. H., and Morel, F. M. M.: Inorganic carbon acquisition in coastal Pacific phytoplankton communities, Limnol. Oceanogr., 45, 1485–1500, doi:10.4319/lo.2000.45.7.1485, 2000.

Tortell, P. D., Payne, C., Gueguen, C., Strzepek, R. F., Boyd, P. W., and Rost, B.: Inorganic carbon uptake by Southern Ocean phytoplankton, Limnol. Oceanogr., 53, 1266–1278, doi:10.4319/lo.2008.53.4.1266, 2008a.

Tortell, P. D., Payne, C. D., Li, Y., Trimborn, S., Rost, B., Smith, W. O. J., Riesselman, C., Dunbar, R. B., Sedwick, P., and DiTullio, G. R.: 10 CO₂ sensitivity of Southern Ocean phytoplankton, Geophys. Res. Lett., 35, L04605, doi:10.1029/2007GL032583, 2008b.

Tortell, P. D., Trimborn, S., Li, Y., Rost, B., and Payne, C. D.: Inorganic carbon utilization by Ross Sea phytoplankton across natural and experimental CO₂ gradients, J. Phycol., 46, 433–443, doi:10.1111/j.1529-8817.2010.00839.x, 2010.

Tortell, P. D., Asher, E. C., Ducklow, H. W., Goldman, J. A. L., Dacey, J. W. H., Grzimski, J. J., Young, J. N., Kranz, S. A., Bernard, K. S., 15 and Morel, F. M. M.: Metabolic balance of coastal Antarctic waters revealed by autonomous pCO₂ and ΔO₂/Ar measurements, Geophys. Res. Lett., 41, 6803–6810, doi:10.1002/2014GL061266, 2014.

Trimborn, S., Brenneis, T., Sweet, E., and Rost, B.: Sensitivity of Antarctic phytoplankton species to ocean acidification: Growth, carbon acquisition, and species interaction, Limnol. Oceanogr., 58, 997–1007, doi:10.4319/lo.2013.58.3.0997, 2013.

Trimborn, S., Thoms, S., Petrou, K., Kranz, S. A., and Rost, B.: Photophysiological responses of Southern Ocean phytoplankton to changes in 20 CO₂ concentrations: Short-term versus acclimation effects, J. Exp. Mar. Bio. Ecol., 451, 44–54, doi:10.1016/j.jembe.2013.11.001, 2014.

van de Waal, D. B., Verschoor, A. M., Verspagen, J. M., van Donk, E., and Huisman, J.: Climate-driven changes in the ecological stoichiometry of aquatic ecosystems, Front. Ecol. Environ., 8, 145–152, doi:10.1890/080178, 2010.

Wang, Y., Zhang, R., Zheng, Q., Deng, Y., Van Nostrand, J. D., Zhou, J., and Jiao, N.: Bacterioplankton community resilience to ocean acidification: evidence from microbial network analysis, ICES J. Mar. Sci. J. du Cons., 73, 865–875, doi:10.1093/icesjms/fsv187, 2016.

Westwood, K., Thomson, P., van den Enden, R., Maher, L., Wright, S., and Davidson, A.: Ocean acidification impacts primary and bacterial 25 production in Antarctic coastal waters during austral summer, J. Exp. Mar. Bio. Ecol., in press.

Westwood, K. J., Brian Griffiths, F., Meiners, K. M., and Williams, G. D.: Primary productivity off the Antarctic coast from 30°–80°E; BROKE-West survey, 2006, Deep Sea Res. Part II Top. Stud. Oceanogr., 57, 794–814, doi:10.1016/j.dsr2.2008.08.020, 2010.

Wright, S. W., van den Enden, R. L., Pearce, I., Davidson, A. T., Scott, F. J., and Westwood, K. J.: Phytoplankton community structure and 30 stocks in the Southern Ocean (30–80°E) determined by CHEMTAX analysis of HPLC pigment signatures, Deep Sea Res. Part II Top. Stud. Oceanogr., 57, 758–778, doi:10.1016/j.dsr2.2009.06.015, 2010.

Wu, Y., Gao, K., and Riebesell, U.: CO₂-induced seawater acidification affects physiological performance of the marine diatom *Phaeodactylum tricornutum*, Biogeosciences, 7, 2915–2923, doi:10.5194/bg-7-2915-2010, 2010.

Young, J., Kranz, S., Goldman, J., Tortell, P., and Morel, F.: Antarctic phytoplankton down-regulate their carbon-concentrating mechanisms 35 under high CO₂ with no change in growth rates, Mar. Ecol. Prog. Ser., 532, 13–28, doi:10.3354/meps11336, 2015.

Zheng, Y., Giordano, M., and Gao, K.: Photochemical responses of the diatom *Skeletonema costatum* grown under elevated CO₂ concentrations to short-term changes in pH, Aquat. Biol., 23, 109–118, doi:10.3354/ab00619, 2015.



Figure 1. Minicoshm tanks filled with seawater in temperature controlled shipping container.

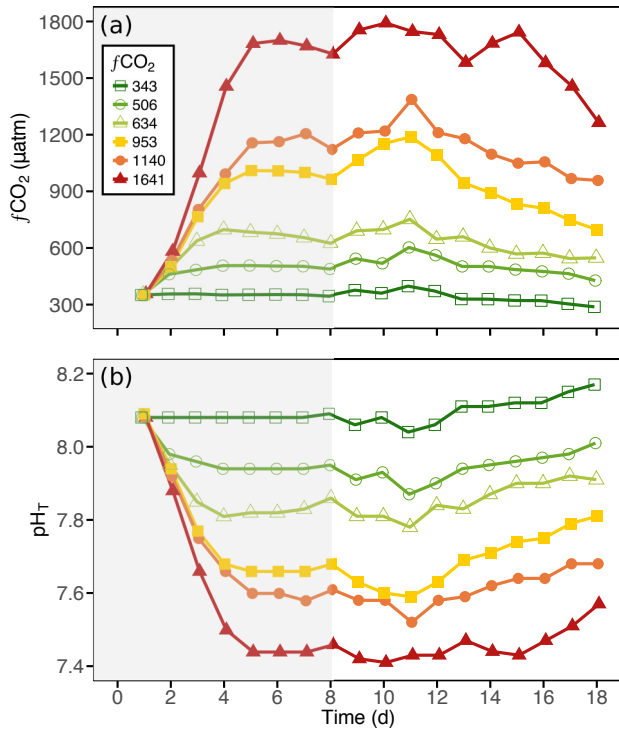


Figure 2. (a) $f\text{CO}_2$ and (b) pH_T conditions within each of the minicomm treatments over time. Grey shading indicates CO_2 and light acclimation period.

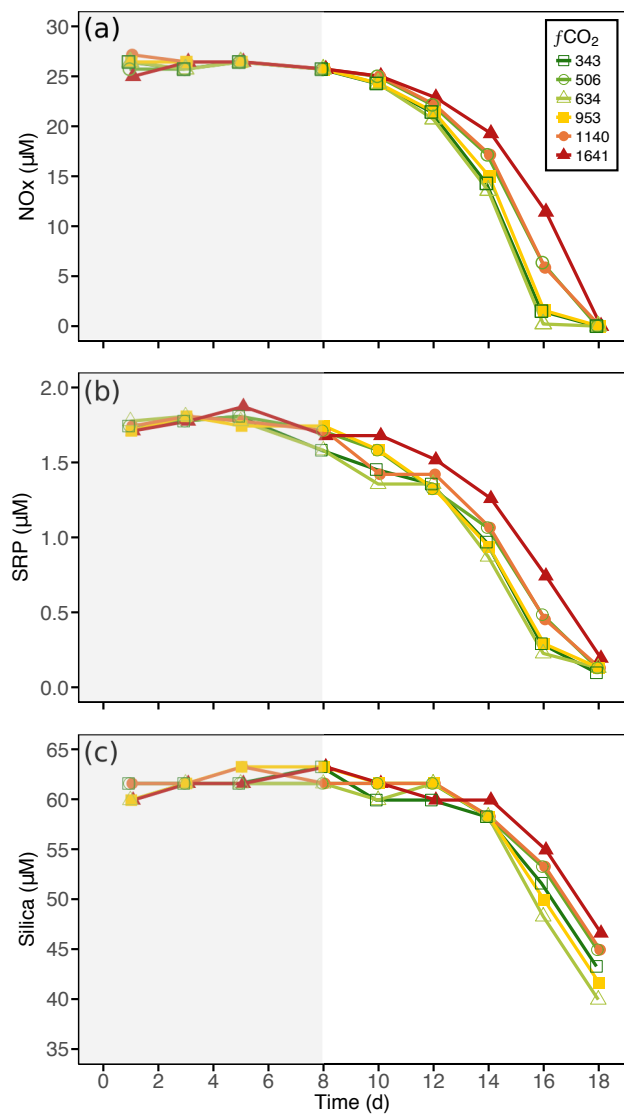


Figure 3. Nutrient concentration in each of the minicomm treatments over time. (a) Nitrate + nitrite (NOx), (b) soluble reactive phosphorus (SRP), and (c) molybdate reactive silica (Silica). Grey shading indicates CO_2 and light acclimation period.

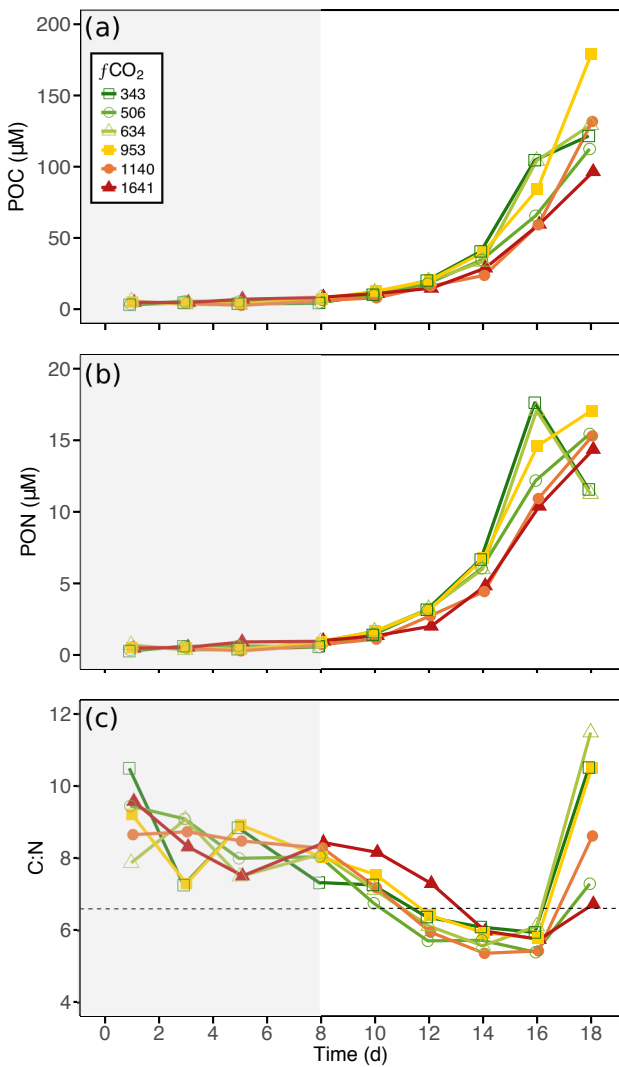


Figure 4. Particulate organic matter concentration and C:N ratio of each of the minicosm treatments over time. (a) Particulate organic carbon (POC), (b) particulate organic nitrogen (PON), and (c) carbon:nitrogen (C:N) ratio. Dashed line indicates C:N Redfield Ratio of 6.6. Grey shading indicates CO₂ and light acclimation period.

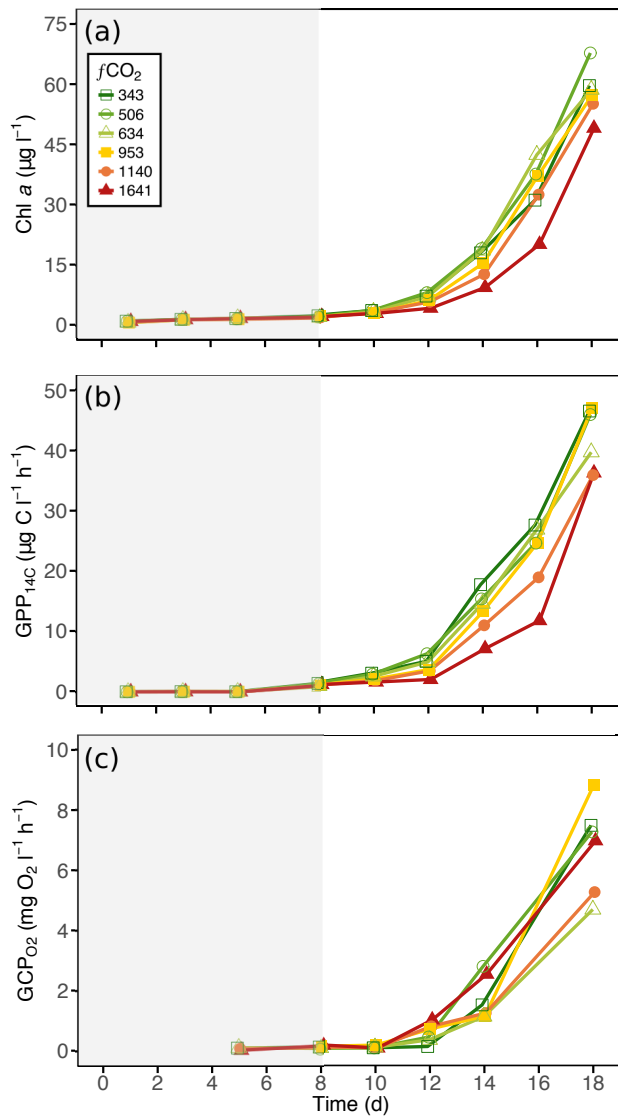


Figure 5. Phytoplankton biomass accumulation and community primary production in each of the minicomm treatments over time. (a) Chlorophyll a (Chl a) concentration, (b) ^{14}C -derived gross primary production ($\text{GPP}_{14\text{C}}$), and (c) O_2 -derived gross community production (GCP_{O_2}). Grey shading indicates CO_2 and light acclimation period.

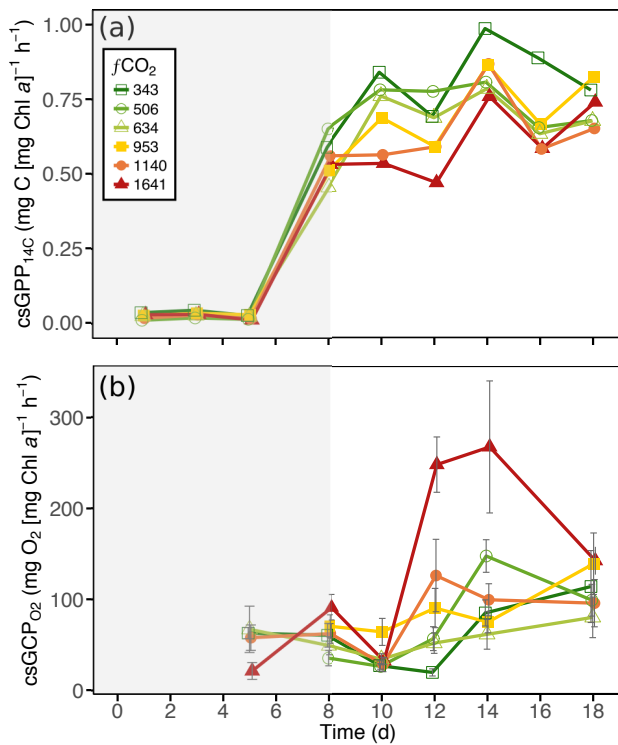


Figure 6. (a) ^{14}C -derived Chl a -specific primary productivity (csGPP $_{14\text{C}}$) and (b) O₂-derived Chl a -specific community productivity (csGCP $_{\text{O}_2}$) in each of the minicommunity treatments over time. Error bars display one standard deviation of pseudoreplicate samples. Grey shading indicates CO₂ and light acclimation period.

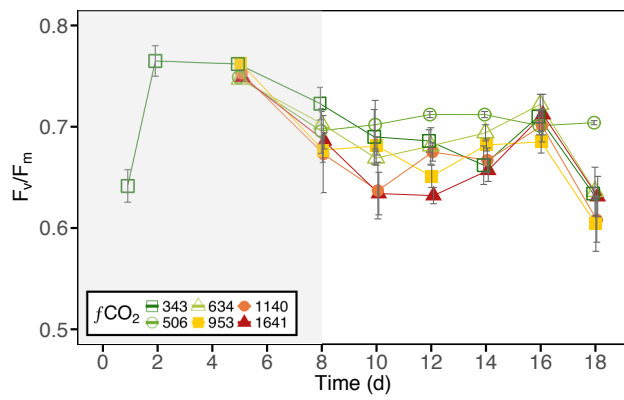


Figure 7. Maximum quantum yield of PSII (F_v/F_m) in each of the minicomm treatments over time. Error bars display one standard deviation of pseudoreplicate samples. Grey shading indicates CO₂ and light acclimation period.

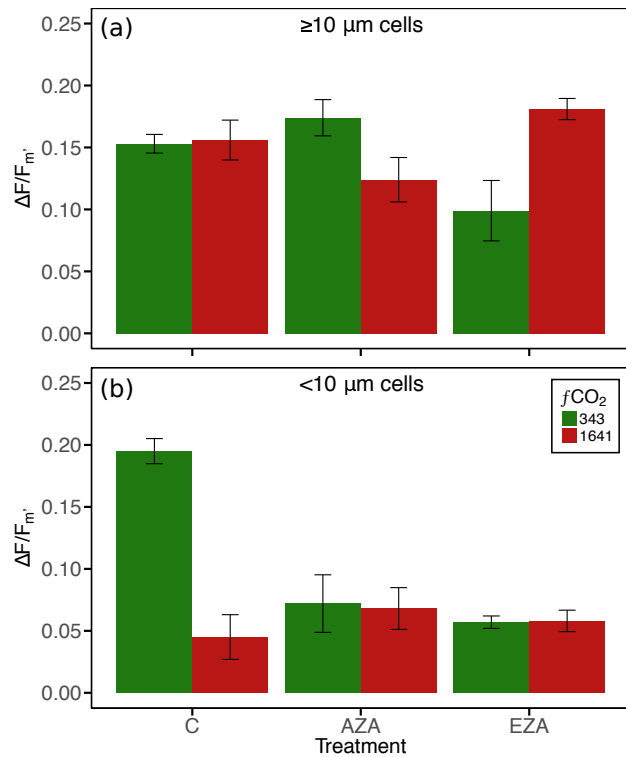


Figure 8. Effective quantum yield of PSII ($\Delta F/F_{m'}$) of (a) large ($\geq 10 \mu\text{m}$) and (b) small ($< 10 \mu\text{m}$) phytoplankton in the control (343 μatm) and high (1641 μatm) CO_2 treatments treated with carbonic anhydrase (CA) inhibitors. A decline in $\Delta F/F_{m'}$ with application of inhibitor indicates CCM activity. C denotes the control treatment, which received no CA inhibitor; AZA is the acetazolamide treatment, which blocks extracellular carbonic anhydrase; EZA is the ethoxzolamide treatment, which blocks intra- and extracellular carbonic anhydrase. Error bars display one standard deviation of pseudoreplicate samples.

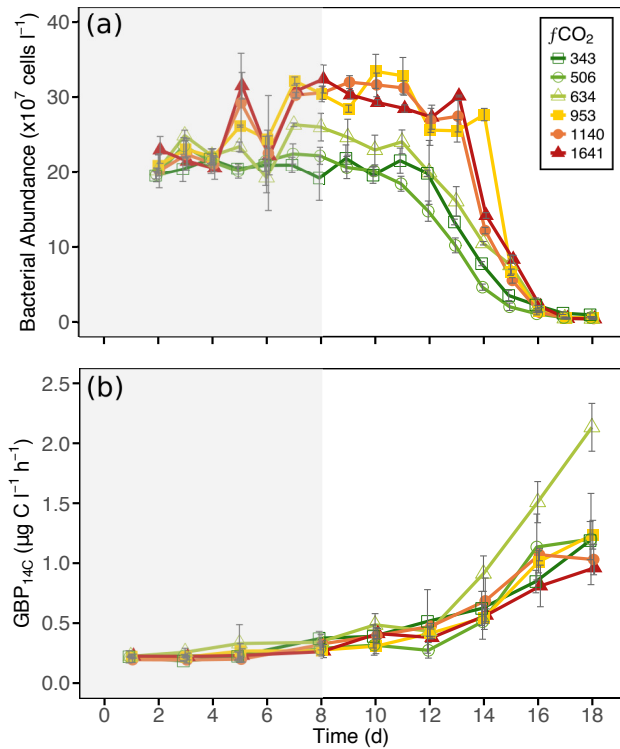


Figure 9. Bacterial abundance and community production in each of the minicosm treatments over time. (a) Bacterial cell abundance and (b) ^{14}C -derived gross bacterial production ($\text{GBP}_{14\text{C}}$). Error bars display one standard deviation of pseudoreplicate samples. Grey shading indicates CO_2 and light acclimation period.

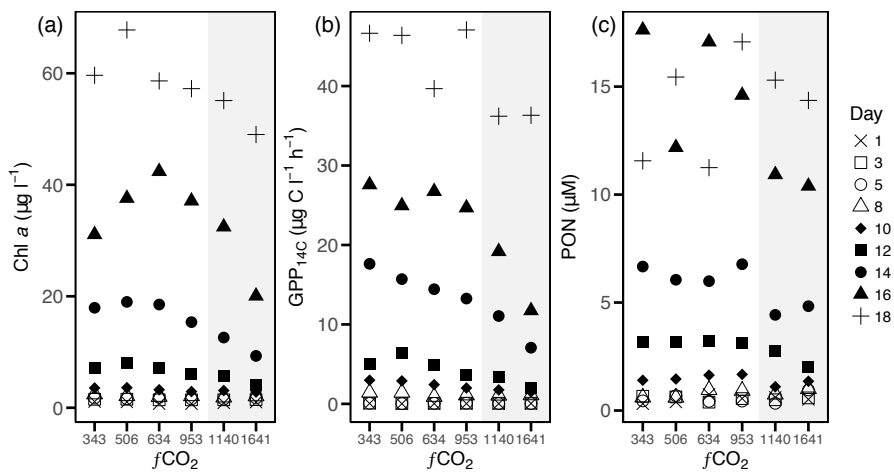


Figure 10. Temporal trends of (a) Chl *a*, (b) ¹⁴C-derived gross primary production (GPP_{14C}), and (c) particulate organic nitrogen (PON) against CO₂ treatment. Grey shading indicates CO₂ treatments $\geq 1140 \mu\text{atm}$.

Table 1. Definitions, measurements and calculations for productivity data

Name	Definition	Units	Measurements and calculations
<i>Primary Productivity</i>			
Carbon incorporation	Total ^{14}C -sodium bicarbonate incorporation	mg C (mg Chl a) $^{-1}$ h $^{-1}$	Equation from Steemann Nielsen (1952)
α	Maximum photosynthetic efficiency	mg C (mg Chl a) $^{-1}$ (μmol photons m $^{-2}$ s $^{-1}$) $^{-1}$ h $^{-1}$	$= \frac{(DPM_s - DPM_{T_0})}{DPM_{100\%}} \times \text{DIC} \times 1.05 / \text{Chl } a$ Modelled from PE curve of 21 light intensities
β	Photoinhibition rate	mg C (mg Chl a) $^{-1}$ (μmol photons m $^{-2}$ s $^{-1}$) $^{-1}$ h $^{-1}$	Modelled from PE curve of 21 light intensities
P_{max}	Maximum photosynthetic rate	mg C (mg Chl a) $^{-1}$ h $^{-1}$	Equation from Platt et al. (1980)
E_k	Saturating irradiance	μmol photons m $^{-2}$ s $^{-1}$	$= P_s \times \frac{\alpha}{(\alpha + \beta)} \times \frac{\beta}{\frac{\alpha}{(\alpha + \beta)}}$ Equation from Platt et al. (1980)
\bar{I}	Average irradiance received by phytoplankton cells	μmol photons m $^{-2}$ s $^{-1}$	Equation from Riley (1957)
$\text{csGPP}_{^{14}\text{C}}$	^{14}C Chl a -specific primary productivity	mg C (mg Chl a) $^{-1}$ h $^{-1}$	$= \bar{I}_o (1 - e^{(-K_d \times Z_m)}) / (K_d \times Z_m)$ Equation from Platt et al. (1980)
$\text{GPP}_{^{14}\text{C}}$	^{14}C gross primary production	$\mu\text{g C l}^{-1} \text{ h}^{-1}$	$= \text{csGPP}_{^{14}\text{C}} \times \text{Chl } a$
$\text{csGCP}_{\text{O}_2}$	O $_2$ Chl a -specific gross community productivity	mg O $_2$ (mg Chl a) $^{-1}$ h $^{-1}$	$= \text{NCP}_{\text{O}_2} + \text{Respo}_{\text{O}_2} / \text{Chl } a$
GCP_{O_2}	O $_2$ gross community production	mg O $_2$ l $^{-1}$ h $^{-1}$	$= \text{csGCP}_{\text{O}_2} \times \text{Chl } a$
<i>Photophysiology</i>			
F_v/F_m	Maximum quantum yield of PSII	(arbitrary units)	$= \frac{F_m - F_O}{F_m}$
$\Delta F/F_{m'}$	Effective quantum yield of PSII	(arbitrary units)	$= \frac{(F_{m'} - F)}{(F_{m'} - F_m)}$
rETR	Relative electron transport rate	(arbitrary units)	$= \frac{\Delta F_v}{\Delta F_{m'}} \times I_a$
NPQ	Non-photochemical quenching	(arbitrary units)	$= \frac{F_{m'} - F_{m'}}{F_{m'}}$
<i>Bacterial Productivity</i>			
$\text{nmol Leucine}_{inc}$	Moles of exogenous ^{14}C -Leucine incorporated	nmol l $^{-1}$ h $^{-1}$	Equation from Kirchman (2001)
$\text{GBP}_{^{14}\text{C}}$	^{14}C gross bacterial production	$\mu\text{g C l}^{-1} \text{ h}^{-1}$	$= (DPM_s - DPM_{T_0}) / \text{time} / 2.22 \times 10^6 \times \text{SA}$ (nmol μCi^{-1}) / sample vol (l)
$\text{csBP}_{^{14}\text{C}}$	^{14}C cell-specific bacterial productivity	fg C cell $^{-1}$ l $^{-1}$ h $^{-1}$	Equation from Simon and Azam (1989)
			$= (\text{nmol Leucine}_{inc} / 10^3) \times 131.2 / 0.073 \times 0.86 \times 2$ = GBP $_{^{14}\text{C}}$ / cells l $^{-1}$

P_s : maximum photosynthetic output with no photoinhibition, from Platt et al. (1980), DPM $_s$: sample DPM, SA: specific activity of ^{14}C -Leucine isotope
All other abbreviations defined in Methods Section